Cancer Immunol Immunother (2004) 53: 1093–1100
DOI 10.1007/s00262-004-0568-y

ORIGINAL ARTICLE

Hideya Onishi · Hideo Kuroki · Kotaro Matsumoto
Eishi Baba · Nobuhiko Sasaki · Hirotaka Kuga
Masao Tanaka · Mitsuo Katano · Takashi Morisaki

Monocyte-derived dendritic cells that capture dead tumor cells secrete IL-12 and TNF-α through IL-12/TNF-α/NF-κB autocrine loop

Received: 3 November 2003 / Accepted: 21 April 2004 / Published online: 18 June 2004

Abstract This study focused on the question of how monocyte-derived dendritic cells (Mo-DCs) that capture dead tumor cells (Mo-DCs-Tum) secrete interleukin 12 (IL-12) and tumor necrosis factor α (TNF-α). Mo-DCs-Tum showed higher secretions of IL-12 and TNF-α than were shown by Mo-DCs. Enhanced nuclear factor-kappa B (NF-κB) activation was also induced in Mo-DCs-Tum within 6 h. The NF-κB inhibitor, pyrrolidine dithiocarbamate (PDTC), suppressed both IL-12 and TNF-α secretions from Mo-DCs-Tum. Administration of recombinant TNF-α or IL-12 enhanced IL-12 or TNF-α secretion respectively in Mo-DCs-Tum. Addition of anti-TNF-α or anti-IL-12 neutralizing antibody decreased NF-κB activation and IL-12 or TNF-α secretion in Mo-DCs-Tum. These results suggest that TNF-α or IL-12 secretion induces NF-κB activation, and it stimulates further TNF-α and IL-12 secretions, i.e., an IL-12/TNF-α/NF-κB autocrine loop, in Mo-DCs-Tum. Thus, Mo-DCs-Tum secrete a large amount of IL-12 and TNF-α through accelerated NF-κB activation induced by the IL-12/TNF-α/NF-κB autocrine loop.

Keywords Dendritic cells · Human · Transcription factors · Tumor immunity

H. Onishi · H. Kuroki · K. Matsumoto · E. Baba · N. Sasaki
H. Kuga · M. Katano · T. Morisaki (✉)
Department of Cancer Therapy and Research,
Graduate School of Medical Sciences,
Kyushu University, Fukuoka,
812-8582, Japan
E-mail: mkatano@tumor.med.kyushu-u.ac.jp
Tel.: +81-92-6426219
Fax: +81-92-6426221

M. Tanaka
Department of Clinical Oncology,
Graduate School of Medical Sciences,
Kyushu University, Fukuoka, Japan

Introduction

Dendritic cells (DCs) play a pivotal role in T and B cell–mediated immune responses [3, 5]. Recent advances in biotechnology have made it possible to generate monocyte-derived DC-like cells (Mo-DCs) in vitro from peripheral blood monocytes with granulocyte-macrophage colony-stimulating factor (GM-CSF) and interleukin 4 (IL-4) [23]. Clinical trials of Mo-DCs pulsed with autologous tumor cells, i.e., Mo-DC–based immunotherapies, are underway for patients with a variety of malignancies including malignant melanoma, B-cell lymphoma, renal cell carcinoma, gastrointestinal carcinoma, and thyroid carcinoma [9, 13, 16, 22, 24]. However, Mo-DC–based tumor immunotherapies have had limited success. One reason is that the level of specific antigen-MHC complexes on tumors may be low and thus only a few T-cell clones that recognize tumor antigens may be activated. It has been shown that Mo-DCs which capture necrotic tumor cells (N) or apoptotic tumor cells (A) become mature, i.e., mature Mo-DCs, and they produce tumor necrosis factor α (TNF-α) and interleukin 12 (IL-12) [3]. Efficient secretion of IL-12 from Mo-DCs is helpful to overcome this problem because Th1-type helper T cells are preferentially induced by IL-12 and play an important role in the antitumor immune response [6, 8]. Unfortunately, IL-12 secretion of Mo-DCs generated from patients with advanced cancer is weaker than that of Mo-DCs from healthy volunteers [18]. These findings indicate that we should prepare Mo-DCs which secrete larger amounts of IL-12 as DC-vaccine source. However, details regarding the molecular mechanism of how Mo-DCs that capture dead tumor cells (Mo-DCs-Tum) secrete IL-12 remain unclear.

Nuclear factor-kappa B (NF-κB) is responsible for maturation of DCs and is a major regulator of the antigen-presenting function of DCs [21]. In resting cells, NF-κB is located in the cytoplasm as heterodimers of the structurally related proteins p50, p52, RelA, c-Rel, and

RelB, both of which are noncovalently associated with the cytoplasmic inhibitor, inhibitory NF-κB (IκB) [17, 25]. Activation of NF-κB is preceded by phosphorylation of IκB by IκB kinase, which is followed by proteolytic removal of IκB and movement of NF-κB to the nucleus. Nuclear translocation of NF-κB is thought to reflect activation of NF-κB [1]. After translocation to the nucleus, NF-κB stimulates transcription of cytokines such as TNF-α and IL-12 [7, 20].

In the present study, we focused on the IL-12 and TNF-α secretions from Mo-DCs-Tum and their molecular mechanism.

Materials and methods

Generation of Mo-DCs

Cultures of human peripheral blood mononuclear cells (PBMCs) were maintained in RPMI 1640 (Sanko Pure Chemicals, Tokyo, Japan) supplemented with 10% fetal bovine serum (FBS; Filtron Pty, Brooklyn, Victoria, Australia), 100 U/ml penicillin (Meijiseika, Tokyo, Japan), and 100 μg/ml of streptomycin (Meijiseika) (hereafter referred to as RPMI medium). Mo-DCs were generated from the adherent fraction of PBMCs as described previously [18] but with minor modifications. In brief, PBMCs were isolated from heparinized peripheral blood from healthy volunteers by Ficol-Paque (Life Technologies, Gaithersburg, MD, USA) density gradient centrifugation. PBMCs were resuspended in RPMI medium, plated at a density of 2×10^6 cells/ml, and allowed to adhere in 24-well culture plates (Nalge Nunk International, Chiba, Japan). After an overnight incubation at 37°C, the nonadherent cells were removed, and the adherent cells were harvested and cultured in RPMI medium supplemented with GM-CSF (200 ng/ml; Genetech, China) and IL-4 (500 U/ml; Osteogenetics, Wuerzburg, Germany). On day 6, nonadherent cell fractions were collected as immature Mo-DCs and examined. In the present study, Mo-DCs from ten healthy donors were prepared and used.

Induction of apoptosis and necrosis in tumor cells

A human gastric carcinoma cell line, GCTM-1, was established in our laboratory and maintained in RPMI medium [15]. Complete disruption of the necrotic cells into fragments was confirmed by light microscopy after five cycles of freezing with liquid nitrogen and thawing at 37°C. UV-triggered apoptosis of tumor cells was induced by 2 mJ/cm^2 of irradiation with a 120-mJ UVB lamp (Amersham Biosciences, Piscataway, NJ, USA). Eight hours after irradiation, induction of apoptosis was confirmed by double staining with Hoechst 33342 (Wako Pure Chemical, Osaka, Japan) and propidium iodide (PI; Sigma, St Louis, MO, USA). Under fluorescence microscopy, PI-negative and Hoechst 33432-positive cells with characteristically condensed or fragmented nuclei were defined as being apoptotic. More than 99% of UV-irradiated GCTM-1 cells had the PI-negative and Hoechst 33432-positive phenotype and typical apoptotic morphology. PI-positive cells were defined as secondary necrotic cells. Necrosis- or apoptosis-induced tumor cell cultures were centrifuged at 6,000 *g* for 10 min, the supernatant was removed, and the pellets were saved. No contamination of LPS into dead tumor cell fraction was confirmed with Limulus amebocyte lysate test (Wako, Tokyo, Japan).

Capture of dead tumor cells by Mo-DCs

Apoptotic or necrotic tumor cells were incubated with Mo-DCs at a cell ratio of 1:1 at 4°C or 37°C. Four hours after incubation, cells were collected, washed with posphate-buffered saline (PBS), and stained with Giemsa (Kokusaishinyaku, Kobe, Japan) to determine the number of Mo-DCs-Tum that captured N (Mo-DCs-Tum-N) or A (Mo-DCs-Tum-A). One hundred Mo-DCs were examined under a light microscope at ×400 magnification, and the percentage of Mo-DCs-Tum (%Mo-DCs-Tum) was calculated. Alternatively, the membrane components of N or A tumor cells were labeled with the PKH 26 red fluorescent cell linker kit (Sigma), and Mo-DCs were labeled with the PKH 67 green fluorescent cell linker kit (Sigma) according to the manufacturer's protocol. Fluorescence-labeled Mo-DCs and dead tumor cells were cocultured at an original cell ratio of 1:1 for 4 h at 4°C or 37°C, washed, and then applied to a FACS Calibur flow cytometer (Becton Dickinson, Franklin Lakes, NJ, USA). The fluorescence intensity was analyzed with CELLQuest software (Becton Dickinson). PKH 26-positive cells in gated Mo-DCs populations were defined as Mo-DCs-Tum-A or Mo-DCs-Tum-N.

Cytokine secretions by Mo-DCs

Ten thousand Mo-DCs and dead tumor cells obtained from 1×10^4 GCTM-1 cells were suspended in 200 μl of RPMI 1640 containing 1% human albumin. Alternatively, these cell mixtures were incubated with or without 1 μg/ml of anti-TNF-α neutralizing IgG (R&D Systems), 200 U/ml of recombinant human TNF-α (Dainippon Pharmaceutical, Osaka, Japan), 20 μg/ml of anti-IL-12 neutralizing IgG (R&D Systems), 100 μg/ml of recombinant IL-12 (Dainippon Pharmaceutical) or 100 μM of pyrrolidine dithiocarbamate (PDTC, Sigma). Twenty-four hours after the initial culture, cell-free supernatants were collected by centrifugation and stored at −80°C until use. The concentrations of IL-12 p40, IL-12 p70, and TNF-α in the culture supernatants were measured by ELISA kit specific for IL-12 p40, IL-12 p70, or TNF-α (Biosource, Camarillo, CA, USA). The detection limit of each kit was 10 pg/ml.

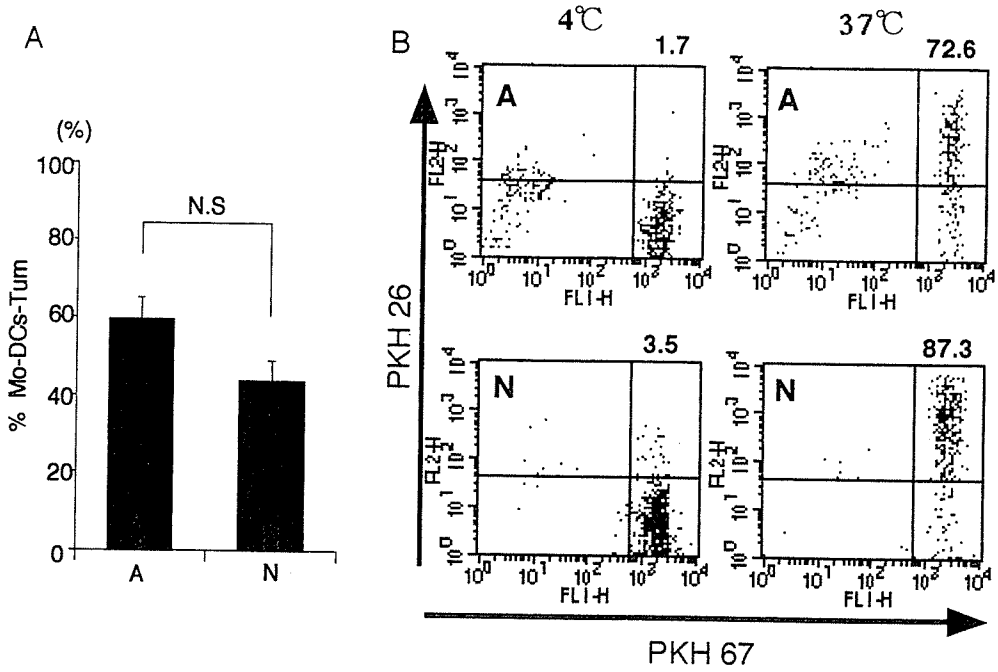

Fig. 1a,b Analysis of dead tumor cells by Mo-DCs. **a** Dead tumor cells were cocultured with an equivalent number of Mo-DCs for 4 h and then stained with Giemsa. One hundred Mo-DCs were examined under a light microscope, and the percentage of Mo-DCs-Tum was calculated (*%Mo-DCs-Tum*). Results are presented as mean ± SE (*bars*). The data are representative of three independent experiments using Mo-DCs generated from ten different donors. **b** Membrane components of dead tumor cells were labeled with PKH 26, and Mo-DCs were labeled with PKH 67. Fluorescence-labeled Mo-DCs were cocultured with dead tumor cells at a ratio of 1:1 for 4 h at 4°C or 37°C. Data are the log fluorescence intensity of Mo-DCs gated by cellular size and granulation phenotype. Fluorescence profiles of Mo-DCs-Tum at 4°C or 37°C are shown. The percentage of double-positive (PKH 26+, PKH 67+) Mo-DCs is shown in the *upper right corner* of each figure. The data are representative of three independent experiments using Mo-DCs generated from three different donors

Preparation of nuclear extract of Mo-DCs

Monocyte-derived dendritic cells cocultured with dead GCTM-1 cells for various durations with or without various agents, including anti-TNF-α neutralizing mAb, anti-IL-12 neutralizing mAb, or PDTC, were collected and washed once with PBS. Cells were then homogenized in 400 µl of hypotonic buffer (10 mM HEPES [pH 7.9], 10 mM KCl, 1.5 mM $MgCl_2$, 0.1% Nonidet P-40, and 5% protease inhibitor cocktail [0.2 mM DTT, 10 mM benzamidine, 7 µg/ml leupeptin, 50 µg/ml soybean trypsin inhibitor, 2 µg/ml aprotinin, 2 µg/ml antipain, 0.7 µg/ml pepstatin, 0.5 mM phenylmethylsulfonyl fluoride, and 0.5 mM 4-(2-aminoethyl) benzenesulfonylfluoride] [Sigma]), and then incubated for 10 min on ice. Nuclei collected by centrifugation at 800 *g* for 5 min were washed once with 200 µl of hypotonic buffer and resuspended in 20 µl of low-salt buffer (20 mM HEPES [pH 7.9], 0.02 mM KCl, 1.5 mM $MgCl_2$, 0.2 mM EDTA, 25% glycerol, and protease inhibitor cocktail). An equal volume of high-salt buffer (same composition as low-salt buffer but containing 800 mM KCl) was added with vortex mixing. Nuclei were incubated for 30 min at 4°C and centrifuged at 18,000 *g* for 30 min, and the supernatants were collected.

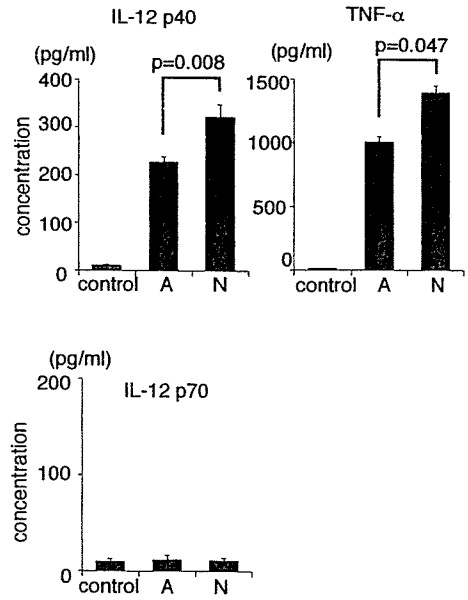

Fig. 2 Secretion of IL-12 p40, TNF-α, and IL-12 p70 by Mo-DCs. Mo-DCs (10^4) were cocultured with 1×10^5 dead GCTM-1 cells for 24 h. Cell-free culture supernatants were collected, and the concentrations of of IL-12 p40, TNF-α, and IL-12 p70 were measured by ELISA ($n=10$). Data are the mean ± SE (*bars*); *p* values for Mo-DCs-Tum-A vs Mo-DCs-Tum-N are listed. The data are representative of two independent experiments using Mo-DCs generated from ten different donors

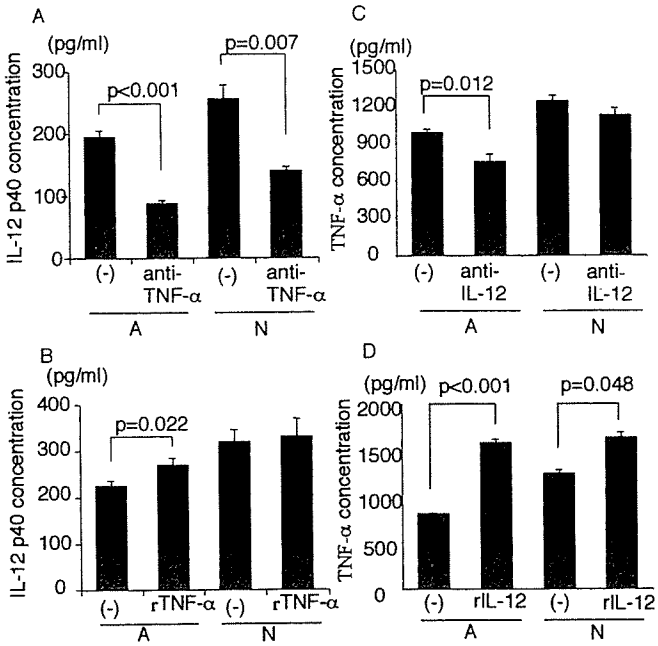

Fig. 3 **a** IL-12 p40 secretion by captured Mo-DCs in the presence of anti-TNF-α neutralizing antibody (1 μg/ml). Mo-DCs (10^4) were cocultured with 1×10^5 dead GCTM-1 cells for 24 h. Cell-free culture supernatants were collected, and the concentration of of IL-12 p40 was measured by ELISA. Data are mean ± SE (*bars*). **b** IL-12 p40 secretion by captured Mo-DCs in the presence of recombinant TNF-α (200 U/ml). Mo-DCs (10^4) were cocultured with 1×10^5 dead GCTM-1 cells for 24 h. Cell-free culture supernatants were collected, and the concentration of of IL-12 p40 was measured by ELISA. Data are mean ± SE (*bars*). **c** TNF-α secretion by Mo-DCs-Tum in the presence of anti-IL-12 (20 μg/ml). Mo-DCs (10^4) were cocultured with 1×10^5 dead GCTM-1 cells for 24 h. Cell-free culture supernatants were collected, and the concentration of TNF-α was measured by ELISA. Data are mean ± SE (*bars*). **d** TNF-α secretion by captured Mo-DCs in the presence of recombinant IL-12 (100 μg/ml). Mo-DCs (10^4) were cocultured with 1×10^5 dead GCTM-1 cells for 24 h. Cell-free culture supernatants were collected, and the concentration of TNF-α was measured by ELISA. Data are mean ± SE (*bars*). The data are representative of three independent experiments using Mo-DCs generated from ten different donors

Electrophoretic mobility shift assay (EMSA)

Nuclear protein extracts of Mo-DCs were analyzed by electrophoretic mobility shift assay (EMSA) for NF-κB nuclear translocation as described previously [11]. Briefly, nuclear protein extracts of 1×10^6 cells were incubated for 30 min at 37°C with binding buffer (60 mM HEPES [pH 7.5], 180 mM KCl, 15 mM $MgCl_2$, 0.6 mM EDTA, and 24% glycerol), poly (dI-dC) (Amersham Pharmacia Biotech AB, Uppsala, Sweden), and ^{32} P-labeled double-stranded oligonucleotide containing the binding motif of NF-κB (5′-AGTTGAGGGGACTTTCCCAGGC-3′) (Promega, Madison, WI, USA). These mixtures were loaded onto a 4% polyacrylamide gel and separated by electrophoresis in 0.25×TBE running buffer. The oligomer-protein complexes were visualized by autoradiography.

Fig. 4 **a** NF-κB activation in Mo-DCs-Tum. Six hours after GCTM-1 cell pulsation, nuclear translocation of NF-κB in Mo-DCs was detected by EMSA. *Lane 1* Mo-DCs (control), *Lane 2* Mo-DCs-Tum-A, *Lane 3* Mo-DCs-Tum-N, *Lane 4* competition assay by the addition of 100 times NF-κB oligonucleotide. Data are the ratio of the intensity of Mo-DCs-Tum to control Mo-DCs as determined by NIH image. **b** NF-κB activation in Mo-DCs-Tum in the presence of anti-TNF-α neutralizing antibody (1 μg/ml). Twelve hours after GCTM-1 cell pulsation, nuclear translocation of NF-κB p65 in Mo-DCs-Tum was analyzed by EMSA. *Lane 1* Mo-DCs-Tum-A, *Lane 2* Mo-DCs-Tum-A in the presence of anti-TNF-α neutralizing antibody, *Lane 3* Mo-DCs-Tum-N, *Lane 4* Mo-DCs-Tum-N in the presence of anti-TNF-α neutralizing antibody. Data are the ratio of Mo-DCs-Tum with anti-TNF-α neutralizing antibody to Mo-DCs-Tum without anti-TNF-α neutralizing antibody as determined by NIH image. **c** NF-κB activation in Mo-DCs-Tum in the presence of anti-IL-12 neutralizing antibody (20 μg/ml). Twelve hours after GCTM-1 cell pulsation, nuclear translocation of NF-κB p65 in Mo-DCs-Tum was analyzed by EMSA. *Lane 1* Mo-DCs-Tum-A, *Lane 2* Mo-DCs-Tum-A in the presence of anti-IL-12 neutralizing antibody, *Lane 3* Mo-DCs-Tum-N, *Lane 4* Mo-DCs-Tum-N in the presence of anti-IL-12 neutralizing antibody. Data are the ratio of Mo-DCs-Tum with anti-IL-12 neutralizing antibody to Mo-DCs-Tum without anti-IL-12 neutralizing antibody as determined by NIH image. The data are representative of three independent experiments using Mo-DCs generated from three different donors

The intensity of the NF-κB band was estimated with the use of NIH Image version 1.60 software (NIH Division of Computer Research and Technology, Bethesda, MD, USA).

Statistical analysis

The Fisher exact probability test was used for statistical analyses. Calculations were carried out with StatView software (Abacus Concepts, Berkeley, CA, USA). All results with a p value less than 0.05 were considered statistically significant.

Results

Mo-DCs capture dead tumor cells

Capture of dead tumor cells by Mo-DCs was essentially determined with Giemsa staining. When the ratio of Mo-DCs-Tum to total Mo-DCs (%Mo-DCs-Tum) was calculated with a light microscope as described in "Materials and methods," %Mo-DCs-Tum was not affected by cellular death pattern, i.e., necrosis or apoptosis, of tumor cells (Fig. 1a). The data are representative of three independent experiments using Mo-DCs generated from ten different donors. Since evaluation with microscopy may be dependent on the investigator's subjective response, %Mo-DCs-Tum was also examined with a flow cytometer. As described in "Materials and methods," Mo-DCs and dead tumor cells were prestained with green fluorescence PKH-67

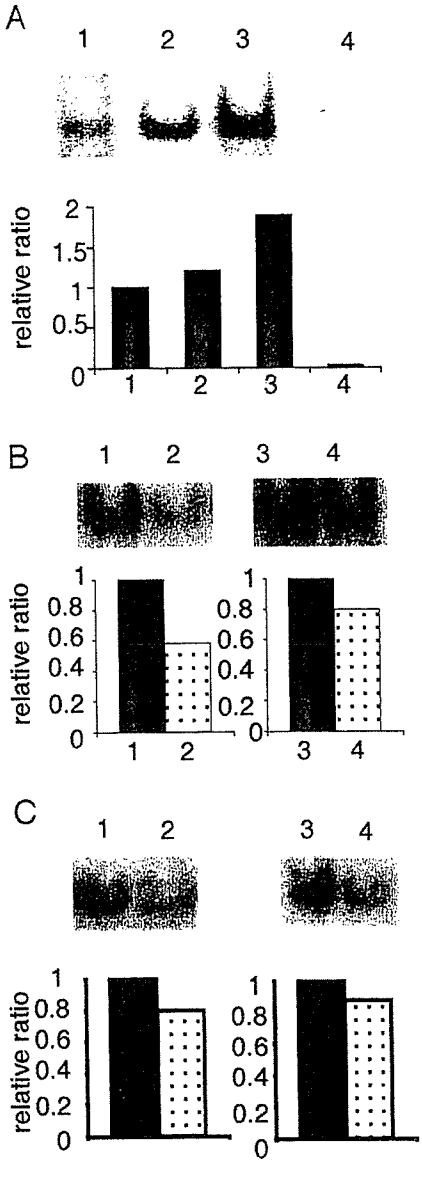

and red fluorescence PKH-26, respectively. As a result, Mo-DCs-Tum become double-positive cells (upper right rectangle in Fig. 1b). The percentage of double-positive cells in Mo-DCs-Tum-N and Mo-DCs-Tum-A was 87.3% and 72.6%, respectively. Uptake was profoundly reduced when dead cells were cocultured with Mo-DCs at 4°C, indicating that nonspecific binding of dead cells to Mo-DCs was minimal (Fig. 1b). The data are representative of three independent experiments using Mo-DCs generated from three different donors. Both Fig. 1a, b, indicate that phagocytotic ability of Mo-DCs was not affected by death pattern of tumor cells.

Mo-DCs-Tum secrete TNF-α and IL-12

We first investigated whether Mo-DCs-Tum secrete IL-12 or TNF-α. Mo-DCs-Tum secreted both TNF-α and IL-12 p40 (Fig. 2). IL-12 p40 secretion (321 ± 26 pg/ml) by Mo-DCs-Tum-N was significantly higher than that (228 ± 10 pg/ml) of Mo-DCs-Tum-A ($p = 0.008$). TNF-α secretion (1,390 ± 60 pg/ml) of Mo-DCs-Tum-N was also significantly higher than that (1,004 ± 42 pg/ml) of Mo-DCs-Tum-A ($p = 0.047$). Concentrations of IL-12 p70 in the culture medium were below the limits of detection in both Mo-DCs-Tum-A and Mo-DCs-Tum-N. These data suggest that the death pattern of tumor cells may affect the production of these cytokines from Mo-DCs-Tum. The data are representative of two independent experiments using Mo-DCs generated from ten different donors.

TNF-α and IL-12 secreted from Mo-DCs-Tum induce further secretion of these cytokines

We next investigated the relationship between TNF-α secretion and IL-12 secretion in Mo-DCs-Tum (Fig. 3). When anti-TNF-α neutralizing antibody was added into the mixture of Mo-DCs and dead tumor cells, IL-12 p40 secretion was significantly decreased (Fig. 3a). Addition of recombinant TNF-α enhanced IL-12 p40 secretion by Mo-DCs-Tum-A but not Mo-DCs-Tum-N (Fig. 3b). Similarly, when anti-IL-12 neutralizing antibody was added into the mixture of Mo-DCs and A, TNF-α secretion was significantly decreased. However, TNF-α secretion by Mo-DCs-Tum-N has not altered significantly (Fig. 3c). Addition of recombinant IL-12 significantly enhanced TNF-α secretion by Mo-DCs-Tum (Fig. 3d). Neither cell viability nor total cell number was changed significantly by the assay (data not shown). These data suggest that TNF-α and IL-12 stimulate each other's cytokine production, i.e., TNF-α/IL-12 autocrine loop. The data are representative of three independent experiments using Mo-DCs generated from ten different donors.

Both IL-12 and TNF-α secreted from Mo-DCs-Tum induce NF-κB activation in Mo-DCs

Since both IL-12 and TNF-α are target genes of NF-κB, induction of NF-κB activation in Mo-DCs-Tum was examined (Fig. 4). NF-κB activation was estimated as translocation of NF-κB p65 to the nuclei of Mo-DCs by EMSA. Enhanced nuclear translocation of NF-κB was observed in Mo-DCs-Tum. Nuclear translocation of NF-κB was stronger in Mo-DCs-Tum-N than Mo-DCs-Tum-A (Fig. 4a). In the presence of anti-TNF-α neutralizing antibody, nuclear translocation of NF-κB in Mo-DCs-Tum was suppressed (Fig. 4b). In the presence of anti-IL-12 neutralizing antibody, nuclear translocation of NF-κB in Mo-DCs-Tum was also suppressed (Fig. 4c). These data suggest the close relationship between TNF-α, IL-12, and NF-κB. The data are representative of three independent experiments using Mo-DCs generated from three different donors.

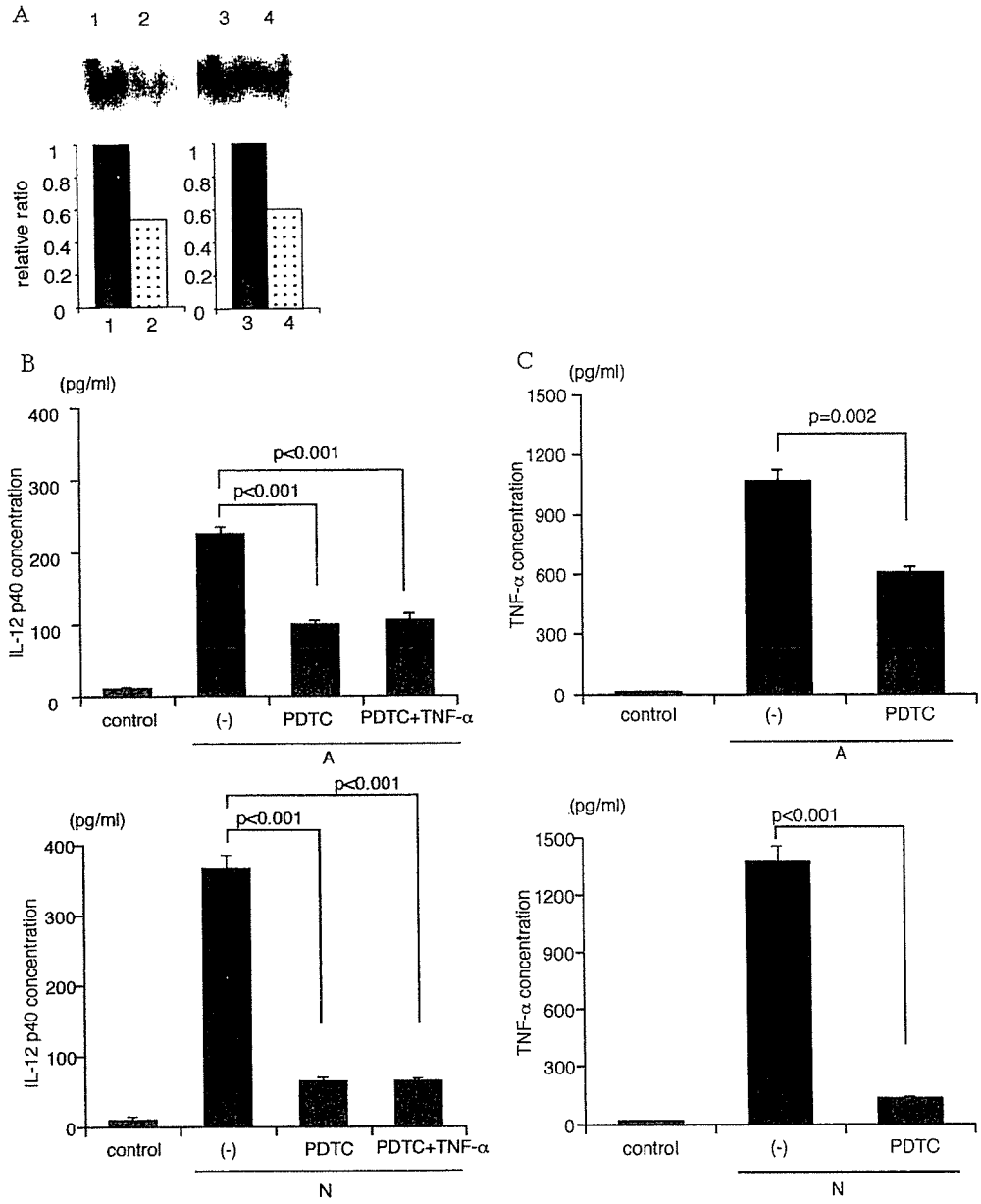

NF-κB inhibitor PDTC suppresses both TNF-α and IL-12 secretion by Mo-DCs-Tum

To confirm the relationship between TNF-α, IL-12, and NF-κB activation, a specific NF-κB inhibitor PDTC was used. In the presence of PDTC, nuclear translocation of NF-κB in Mo-DCs-Tum was certainly suppressed (Fig. 5a). The data are representative of three independent experiments using Mo-DCs generated from three different donors. IL-12 p40 secretion by Mo-DCs-Tum in the presence of PDTC was decreased significantly in comparison to that of Mo-DCs cultured in the absence of PDTC (Fig. 5b; $p < 0.001$). The data are representative of three independent experiments using Mo-DCs generated from ten different donors. Addition of recombinant TNF-α could not ameliorate the decreased IL-12 secretion in PDTC-treated Mo-DCs-Tum (Fig. 5b). Similarly, TNF-α secretion by Mo-DCs-Tum-N or Mo-DCs-Tum-A in the presence of PDTC was decreased significantly in comparison with that in the absence of PDTC ($p < 0.001$ and $p = 0.002$, respectively; Fig. 5c). The data are representative of three independent experiments using Mo-DCs generated from ten different donors. These data indicate the TNF-α/IL-12 / NF-κB autocrine loop in Mo-DCs-Tum.

Discussion

We showed that Mo-DCs-Tum secrete considerable amounts of IL-12 and TNF-α through the IL-12/TNF-α/NF-κB autocrine loop.

◀

Fig. 5 **a** NF-κB activation in Mo-DCs-Tum in the presence of 100 μM of PDTC. Six hours after the GCTM-1 cell pulsation, nuclear translocation of NF-κB in Mo-DCs was examined by EMSA. *Lane 1* Mo-DCs-Tum-A, *Lane 2* Mo-DCs-Tum-A treated with 100 μM PDTC, *Lane 3* Mo-DCs-Tum-N, *Lane 4* Mo-DCs-Tum-N treated with 100 μM PDTC. Data are the ratio of Mo-DCs-Tum in the presence of PDTC to Mo-DCs-Tum in the absence of PDTC as calculated by NIH image. The data are representative of three independent experiments using Mo-DCs generated from three different donors. **b** IL-12 p40 secretion by Mo-DCs-Tum treated with 100 μM of PDTC with or without 200 U/ml of recombinant TNF-α. Mo-DCs (10^4) were cocultured with 1×10^5 dead GCTM-1 cells for 24 h. Cell-free culture supernatants were collected, and the concentration of TNF-α was measured by ELISA. Data are mean ± SE (*bars*). The data are representative of three independent experiments using Mo-DCs generated from ten different donors. **c** TNF-α secretion by Mo-DCs-Tum in the presence of 100 μM of PDTC. Mo-DCs (10^4) were cocultured with 1×10^5 dead GCTM-1 cells for 24 h. Cell-free culture supernatants were collected, and the concentration of TNF-α was measured by ELISA. Data are mean ± SE (*bars*). The data are representative of three independent experiments using Mo-DCs generated from ten different donors

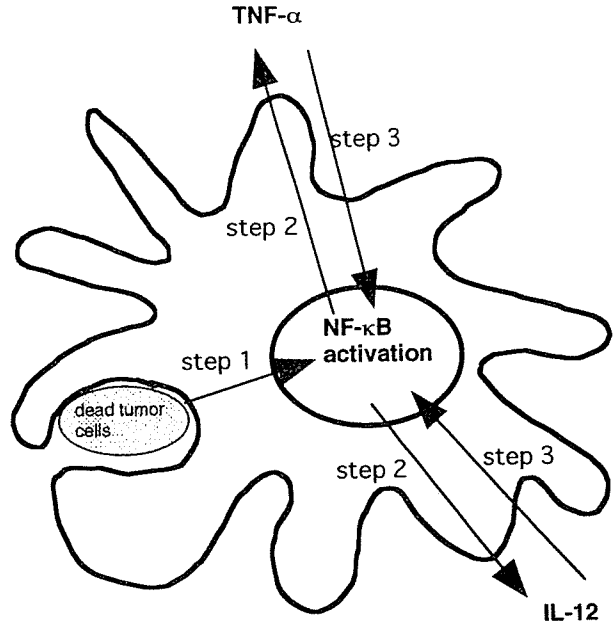

Fig. 6 Possible model of IL-12 and TNF-α secretions through IL-12/TNF-α/NF-κB autocrine loop. NF-κB activation is induced in Mo-DCs-Tum (*step 1*). NF-κB activation induces secretion of both TNF-α and IL-12 (*step 2*). Both IL-12 and TNF-α secretions induce further NF-κB activation (*step 3*). Enhanced NF-κB activation induces further secretion of IL-12 and TNF-α. Thus, IL-12, TNF-α, and NF-κB form an autocrine loop in Mo-DCs-Tum

We first showed a possibility that TNF-α secreted from Mo-DCs-Tum induces further IL-12 secretion from them, and similarly IL-12 secreted from captured Mo-DCs induces further TNF-α secretion from them (Fig. 3). These findings lead to speculation regarding the existence of a TNF-α/IL-12 autocrine loop in Mo-DCs-Tum. Antibodies against TNF-α or IL-12, however, could not completely suppress the secretion of these cytokines. In addition, recombinant TNF-α did not induce significant IL-12 secretion from Mo-DCs-Tum-N. Therefore, our data also indicate that some other mechanisms different from the TNF-α/IL-12 autocrine loop play roles in cytokine secretion from Mo-DCs-Tum. Why do Mo-DCs-Tum secrete both TNF-α and IL-12? It has been shown that transcription of TNF-α is regulated by NF-κB activation [20] and that TNF-α acts in an autocrine manner to induce NF-κB activation in Mo-DCs [23]. In addition, it has been reported that IL-12 secretion of DCs from mice with a double knockout of the NF-κB subunits p50 and cRel was impaired [19]. IL-12 is also a target gene of NF-κB in humans [7]. These data indicate that NF-κB activation plays a key role in secretion of both TNF-α and IL-12 in Mo-DCs-Tum. This possibility may be strongly supported by data showing that an NF-κB inhibitor, PDTC, significantly reduced secretion of both TNF-α and IL-12 in Mo-DCs-Tum (Fig. 5). The next question is what the initial NF-κB activation factor is. Many factors such as lipopolysaccharides, microbial stimuli, viral infection, proinflammatory cytokines, double-stranded DNA, and heat shock proteins (HSPs) have been reported to be activators of NF-κB [2, 4, 10, 14, 26–28]. We have shown that both secretion of IL-12 and activation of NF-κB induced by a streptococcal preparation OK-432 were suppressed when Mo-DCs were pretreated with an inhibitor of endocytosis, cytochalasin B [12], suggesting a possibility that NF-κB activation may be induced in Mo-DCs by capture of dead tumor cells. We are now speculating on at least two possibilities. One possibility is that capture of dead tumor cells induces first TNF-α secretion and then TNF-α secretion stimulates NF-κB activation. Another possibility is that the capture of dead tumor cells directly induces NF-κB activation.

In conclusion, it seems likely that captured Mo-DCs secrete a large amount of IL-12 and TNF-α through the IL-12/TNF-α/NF-κB autocrine loop (Fig. 6). Briefly, NF-κB activation is induced in Mo-DCs-Tum (step 1). NF-κB activation induces secretions of both TNF-α and IL-12 (step 2). Both IL-12 and TNF-α secretions induce further NF-κB activation (step 3). Enhanced NF-κB activation induces further secretion of IL-12 and TNF-α. Thus, IL-12, TNF-α, and NF-κB form an autocrine loop in Mo-DCs-Tum. Such an enhanced NF-κB activation in Mo-DCs-Tum induces them to secrete a large amount of IL-12 and TNF-α. However, it is still unknown to what degree the IL-12/TNF-α/NF-κB autocrine loop plays a role in IL-12 and TNF-α secretions from Mo-DCs-Tum. Identification of an initial signal or key molecule (step 1 in Fig. 6) operating the IL-12/TNF-α/NF-κB autocrine loop might provide new insights that could foster development of an effective antitumor immunotherapy.

Acknowledgements This study was supported by a Grant-in-Aid for General Scientific Research (12557106 and 13470240) from the Ministry of Education, Culture, Sports, Science, and Technology of Japan. We thank Kaori Nomiyama for skillful technical assistance.

References

1. Baeuerle PA, Henkel T (1994) Function and activation of NF-κB in the immune system. Annu Rev Immunol 12:141
2. Baldwin AS Jr (1996) The NF-κB and IκB proteins; new discoveries and insights. Annu Rev Immunol 14:649
3. Banchereau J, Steinman RM (1998) Dendritic cells and the control of immunity. Nature 392:245
4. Basu S, Binder RJ, Suto R, Anderson KM, Srivastava PK (2000) Necrotic but not apoptotic cell death release heat shock proteins, which deliver a partial maturation signal to dendritic cells and activate the NF-κB pathway. Int Immunol 12:1539
5. Cella M, sallusto F, Lanzavecchia A (1997) Origin, maturation and antigen presenting function of dendritic cells. Curr Opin Immunol 9:10
6. Gerosa F, Paganin C, Peritt D, Paiola F, Scupoli MT, Amezaga MA, Frank I, Trinchieri G (1996) Interleukin-12 primes human CD4 and CD8 T cell clones for high secretion of both interferon-γ and interleukin-10. J Exp Med 183:2559
7. Grohmann U, Belladonna ML, Bianchi R, Orabona C, Ayroldi E, Fioretti MC, Puccetti P (1998) IL-12 acts directly on DC to promote nuclear localization of NF-κB and primes DC for IL-12 secretion. Immunity 9:315
8. Heufler C, Koch F, Stanzl U, Topar G, Wysocka M, Trinchieri G, Enk A, Steinman RM, Romani N, Schuler G (1996) Interleukin-12 is produced by dendritic cells and mediates T helper 1 development as well as interferon-g production by T helper 1 cells. Eur J Immunol 26:659
9. Hsu F, Benike C, Fagnoni F, Liles T, Czerwinski D, Taidi B, Engleman E, Levy R (1996) Vaccination of patients with B-cell lymphoma using autologous antigen-pulsed dendritic cells. Nat Med 2:52
10. Ishi K, Suzuki K, Coban C, Takeshita F, Itoh Y, Matoba H, Kohn LD, Klinman DM (2001) Genomic DNA released by dying cell induces the maturation of APCs. J Immunol 167:2602
11. Kojima H, Morisaki T, Izuhara K, Uchiyama A, Matsunari Y, Katano M, Tanaka M (2000) Lipopolysaccharide increases cyclo-oxygenase-2 expression in a colon carcinoma cell line through nuclear factor-κB activation. Oncogene 19:1225
12. Kuppner MC, Gastpar R, Gelwer S, Nossner E, Ochmann O, Scharner A, Issels RD (2001) The role of heat shock protein (hsp 70) in dendritic cell maturation: HSP70 induces the maturation of immature dendritic cells but reduces DC differentiation from monocyte precursors. Eur J Immunol 31:1602
13. Kuroki H, Morisaki T, Matsumoto K, Onishi H, Baba E, Tanaka M, Katano M (2003) Streptococcal preparation OK-432: a new maturation factor of monocyte-derived dendritic cells for clinical use. Cancer Immunol Immunother 52(9):561–568
14. Marten A, Flieger D, Renoth S, Weineck S, Albers P, Compes M, Schottker B, Ziske C, Engelhart S, Hanfland P, Krizek L, Faber C, von Ruecker A, Muller S, Sauerbruch T, Schmidt-Wolf IG (2002) Therapeutic vaccination against metastatic renal cell carcinoma by autologous dendritic cells: preclinical results and outcome of a first clinical phase I/II trial. Cancer Immunol Immunother 51:637
15. Morisaki T, Matsunaga H, Beppu K, Ihara E, Hirano K, Kanaide H, Mori M, Katano M (2000) A combination of cyclosporin-A (CsA) and interferon-γ induces apoptosiss in human gastric carcinoma cells. Anticancer Res 20:3363
16. Nestle F, Alijagic S, Gilliet M, Sun Y, Grabbe S, Dummer R, Burg G, Schadendorf D (1998) Vaccination of melanoma patients with peptide- or tumor lysate- pulsed dendritic cells. Nat Med 4:328
17. Neumann M, Marienfeld R, Serfling E (1997) Rel/NF-κB transcription factors and cancer; oncogenesis by dysregulated transcription. Int J Oncol 11:1335
18. Onishi H, Morisaki T, Baba E, Kuga H, Kuroki H, Matsumoto K, Tanaka M, Katano M (2002) Dysfunctional and short-lived subsets in monocyte-derived dendritic cells from patients with advanced cancer. Clin Immunol 105:286
19. Ouaaz F, Arron J, Zheng Y, Choi Y, Beg AA (2002) Dendritic cell development and survival require distinct NF-κB subunits. Immunity 16:257
20. Prieschl EE, Pendl GG, Elbe A, Serfling E, Harrer NE, Stingl G, Baumruker T (1996) Induction of the TNF-α promoter in the murine dendritic cell line 18 and the murine mast cell line CPII is differently regulated. J Immunol 157:2645
21. Rescigno M, Martino M, Sutherland CL, Gold MR, Castagnoli PR (1998) Dendritic cell survival and maturation are regulated by different signaling pathways. J Exp Med 188:2175
22. Sadanaga N, Nagashima N, Mashino K, Tahara K, Yamaguchi H, Ohta M, Fujie T, Tanaka F, Inoue H, Takesako K, Akiyoshi T, Mori M (2001) Dendritic cell vaccination with MAGE peptide is a novel therapeutic approach for gastrointestinal carcinomas. Clin Cancer Res 7:2277
23. Sallusto F, Lanzavecchia A (1994) Efficient presentation of soluble antigen by cultured human dendritic cells is maintained by granulocyte/macrophage colony-stimulating factor plus interleukin 4 and downergulated by tumor necrosis factor α. J Exp Med 179:1109
24. Schott M, Seissler J, Lettmann M, Fouxon V, Scherbaum WA, Feldkamp J (2001) Immunotherapy for medullary thyroid carcinoma by dendritic cell vaccination. J Clin Endocrinol Metab 86:4965
25. Thanos D, Maniatis T (1995) A lesson in family values. Cell 80:529
26. Todryk S, Melcher AA, Hardwick N, Linardakis E, Bateman A, Colombo MP, Stoppacciaro A, Vile RG (1999) Heat shock protein 70 induced during tumor cell killing induces Th1 cytokines and targets immature dendritic cell precursor to enhance antigen uptake. J Immunol 163:1398
27. Vabulas RM, Braedel S, Hilf N, Singh-Jasuja H, Herter S, Ahmad-Nejad P, Kirschning CJ, Da-Costa C, Rammensee HG, Wagner H, Schild H (2002) The endoplasmic reticulum-resident heat shock protein Gp96 activates dendritic cells via the Toll-like receptor 2/4 pathway. J Biol Chem 277:20847
28. Zheng H, Dai J, Stoilova D, Li Z (2001) Cell surface targeting of heat shock protein gp96 induces dendritic cell maturation and antitumor immunity. J Immunol 167:6731

Available online at www.sciencedirect.com
SCIENCE DIRECT®
Cellular Immunology 231 (2004) 20–29
Cellular Immunology
www.elsevier.com/locate/ycimm

Exosomes secreted from monocyte-derived dendritic cells support in vitro naive CD4$^+$ T cell survival through NF-κB activation☆

Kotaro Matsumoto[a,1], Takashi Morisaki[a], Hideo Kuroki[a], Makoto Kubo[a], Hideya Onishi[a], Katsuya Nakamura[a], Chihiro Nakahara[a], Hirotaka Kuga[a], Eishi Baba[a], Masafumi Nakamura[a], Kazuho Hirata[b], Masao Tanaka[c], Mitsuo Katano[a,*]

[a] *Department of Cancer Therapy and Research, Graduate School of Medical Sciences, Kyushu University, Fukuoka, Japan*
[b] *Department of Anatomy and Cell Biology, Graduate School of Medical Sciences, Kyushu University, Fukuoka, Japan*
[c] *Department of Surgery and Oncology, Graduate School of Medical Sciences, Kyushu University, Fukuoka, Japan*

Received 9 August 2004; accepted 4 November 2004
Available online 11 January 2005

Abstract

We investigated the effect of exosomes secreted from human monocyte-derived dendritic cells (Mo-DCs), which are generated from PBMCs in response to treatment with GM-CSF and IL-4, on naive CD4$^+$ T cell survival in vitro. Exosomes isolated from culture supernatants of Mo-DCs (>90% purity) were purified with anti-HLA-DP, -DQ, -DR-coated paramagnetic beads. Purified exosomes prolonged the survival of naive CD4$^+$ T cells (>98% purity) in vitro. Treatment with neutralizing mAb against HLA-DR significantly decreased the supportive effect of purified exosomes on CD4$^+$ T cell survival. Exosomes increased nuclear translocation of NF-κB in naive CD4$^+$ T cells, and NF-κB activation was significantly suppressed by anti-HLA-DR mAb or NF-κB inhibitor pyrrolidine dithiocarbamate (PDTC). In addition, PDTC inhibited the effect of exosomes on naive CD4$^+$ T cell survival. Thus, exosomes secreted by Mo-DCs appear to support naive CD4$^+$ T cell survival via NF-κB activation induced by interaction of HLA-DR and TCRs.

Keywords: Human monocyte-derived dendritic cells; Multivesicular body; Small membrane vesicle; TCR and MHC interaction

1. Introduction

Prolonged survival of naive CD4$^+$ T cells requires direct contact with self-MHC class II ligands in vivo [1–3]. CD8$^+$ T cells also require exposure to specific self-MHC class I proteins for prolonged survival [4]. Thus, interaction between TCR and MHC molecules plays an important role in supporting naive T cell survival in vivo [5,6]. However, there are few reports concerning the role of TCR and MHC interaction in short-term survival of naive CD4$^+$ T cells in vitro [7].

Exosomes were initially described as microvesicles containing 5′-nucleotidase activity and released from neoplastic cell lines [8,9]. Electron microscopy has shown that exosomes have a characteristic saucer-like morphology of a flattened sphere limited by a lipid bilayer. They range from 30 to 100 nm in diameter [10]. The most common procedure for purifying exosomes from cell-culture supernatants involves a series of centrifugations to remove dead cells and large debris, followed by a final high-speed ultracentrifugation to pellet the exosomes [11,12]. It is generally believed that exosomes are

☆ This work is supported in part by a Grant for Scientific Research (13470240) from the Ministry of Education, Science and Culture, Japan.
* Corresponding author. Fax: +81 92 642 6221.
E-mail address: mkatano@tumor.med.kyushu-u.ac.jp (M. Katano).
[1] Present address: Department of Surgery and Oncology, Graduate School of Medical Sciences, Kyushu University, Fukuoka, Japan.

0008-8749/$ - see front matter © 2004 Elsevier Inc. All rights reserved.
doi:10.1016/j.cellimm.2004.11.002

membrane vesicles that form within late endocytic compartments, multivesicular bodies (MVBs), and are secreted upon fusion of these compartments with the plasma membrane of living cells. As a result, all exosomal proteins reported up to now have been found in the cytosol, in the membrane of endocytic compartments, or at the plasma membrane. Various cell types secrete exosomes. APCs such as dendritic cells (DCs)[2] and B cells also secrete exosomes. Recent advances in biotechnology have made it possible to generate DC-like cells, monocyte-derived DCs (Mo-DCs), in vitro from PBMCs upon treatment with GM-CSF and IL-4 [13], and Mo-DCs secrete exosomes [14]. MHC class II proteins are very abundant in exosomes from Mo-DCs as well as other APCs [15]. In addition, APC-derived exosomes contain specific proteins, such as CD86 and integrins, which are involved in antigen presentation, suggesting a role of exosomes in T cell stimulation [16–18]. In fact, it has been shown that EBV-transformed B cell-derived exosomes stimulate human $CD4^+$ T cell clones in an antigen-specific manner [10]. T cell stimulation by exosomes produced by rat mast cells engineered to express mouse or human MHC class II proteins has been reported [19]. Interestingly, exosomes produced by tumor peptide-pulsed DCs induce T cell-dependent tumor rejection in vivo [14].

NF-κB is a transcription factor that is activated in T cells by interaction between TCRs and MHC class I or class II proteins [20–22] and has been shown to play an important role in the expression of anti-apoptotic genes [23]. In most resting cells, NF-κB is located in the cytoplasm as a heterodimer of the structurally related proteins p50, p52, RelA, c-Rel, and RelB. All of these are noncovalently associated with the cytoplasmic inhibitor IκB [24]. The most common NF-κB is the p65/p50 heterodimer. Activation of NF-κB is preceded by phosphorylation of IκB by IκB kinase, which is followed by proteolytic removal of IκB and movement of NF-κB to the nucleus. Nuclear translocation of NF-κB is thought to reflect its activation [25]. Zheng et al [26] reported a critically important function of NF-κB in TCR-induced regulation of $CD4^+$ T cell survival in p50−/− cRel−/− mice. In addition, survival of antigen-stimulated T cells requires NF-κB-mediated inhibition of p73 expression [22]. Thus a role of NF-κB in T cell survival appears to be important. However, a role of the NF-κB-activating pathway in naive $CD4^+$ T cell survival has not been identified in human cells.

Here, we report for the first time that Mo-DC-derived exosomes support naive $CD4^+$ T cell survival in vitro through interaction between TCRs and human leukocyte antigen (HLA)-DR, and that TCR-dependent NF-κB activation may contribute to this survival.

2. Materials and methods

2.1. Reagents

Pyrrolidine dithiocarbamate (PDTC), an inhibitor of NF-κB nuclear translocation, was purchased from Sigma Chemical (Deisenhofen, Germany).

2.2. Preparation of human Mo-DCs and naive $CD4^+$ T cells

Mo-DCs were generated from the adherent fraction of PBMCs from healthy volunteers, as previously described but with minor modifications [13]. Briefly, PBMCs were isolated from heparinized peripheral blood by Ficol–Paque (Life Technologies, Gaithersburg, MD, USA) density gradient centrifugation. PBMCs were resuspended in RPMI 1640 basal medium (Sanko Pure Chemicals, Tokyo Japan) supplemented with 1% human albumin (Mitsubishi Pharma, Osaka, Japan), 100 μg/ml penicillin (Meijiseika, Tokyo, Japan), and 100 μg/ml streptomycin (Meijiseika) (RPMI medium), plated at a density of 2×10^6 cells/ml, and allowed to adhere overnight at 37 °C in 24-well plates (Nalge Nunc International, Chiba, Japan). Nonadherent cells were removed, and adherent cells were cultured in RPMI medium containing GM-CSF (100 ng/ml, North China Pharmaceutical Group, Shijiazhuang, China) and IL-4 (50 ng/ml, Osteogenetics, Wurzburg, Germany). On day 7, nonadherent fractions were collected as Mo-DCs. Mo-DCs were further purified by negative selection with magnetic beads coated with mouse monoclonal anti-CD2, anti-CD3, and anti-CD19 antibodies (Dynabeads, Dynal Biotech, Oslo, Norway). This depletion procedure yielded over 90% $CD14^-$, $CD80^+$, and $HLA\text{-}DR^+$ Mo-DCs as assessed by fluorescence-activated cell sorting (FACS) (FACS Calibur flow cytometer, Becton–Dickinson Immunocytochemistry Systems, Franklin Lakes, NJ, USA) and analyzed with CELLQuest software (Becton–Dickinson).

Seven days after the initial culture of nonadherent cells, PBMCs were collected again from the same healthy volunteer. $CD4^+$ T cells were purified from fresh human PBMCs with a CD4-positive isolation kit (Dynabeads, Dynal Biotech) according to the manufacturer's instructions. This positive-selection process yielded over 98% $CD4^+$ T cells.

Fresh $CD4^+$ T cells and Mo-DCs isolated from the same healthy volunteer were used throughout this study.

[2] *Abbreviations used:* DC, dendritic cell; Mo-DC, monocyte-derived dendritic cell; PDTC, pyrrolidine dithiocarbamate; MVB, multivesicular body; CB, cacodylate buffer; MW, molecular weight; FSC, forward scatter; SSC, side scatter.

2.3. Exosome isolation and purification

Mo-DCs were generated from PBMCs with GM-CSF and IL-4 as described above. Seven days after the initiation of culture, Mo-DC culture supernatants were collected. Exosomes were isolated as previously described but with minor modifications [11,12]. Culture supernatants were centrifuged at 300*g* for 5 min and then at 1200*g* for 20 min to eliminate cells and debris. Cell-free supernatants were clarified through a 0.2-μm filter (Sartorius AG, Goettingen, Germany) to reduce the number of contaminating large vesicles shed from the plasma membrane. The clarified supernatant was subsequently concentrated through a 100-kDa membrane (YM-100, Microcon, Millipore, Billerica, MA, USA). In some experiments, this concentration procedure was repeated five times with PBS (Wako Pure Chemical Industries, Osaka, Japan) to eliminate the original culture supernatant. The concentrated materials were resuspended in RPMI medium at the original volume of the supernatant. This preparation was denoted crude exosomes.

Exosomes were further purified with human anti-HLA-DP, -DQ, or -DR-coated paramagnetic beads (average size: 4.5 μm, Dynal). Briefly, human anti-HLA-DP, -DQ, or -DR-coated paramagnetic beads were washed with PBS. And 1.0×10^6 DC-derived exosomes were mixed with 1.0×10^6 paramagnetic beads. The mixture was incubated at 4 °C for 24 h on a rotating plate, and the beads were washed twice on a magnetic rack with PBS containing 3% BSA (Sigma) and 0.1% NaN_3 (Sigma) (referred to as FACS buffer) to eliminate unbound or excess exosomes. Finally, exosomes coupled to the beads were resuspended in RPMI medium at the original volume of the exosome-containing medium. This preparation was denoted purified exosomes.

2.4. Naive $CD4^+$ T cell culture

$CD4^+$ T cells were suspended at a cell density of 1.0×10^6/ml, and 1.5×10^5 $CD4^+$ T cells were plated in a 96-well flat-bottomed culture plate (150 μl) and cultured at 37 °C for the indicated times. In an experiment using separated cell-culture system, $CD4^+$ T cells (1.5×10^6 cells) were cultured with Mo-DCs (1.5×10^5 cells) in 1.5 ml of RPMI medium or were cultured separately in RPMI medium (1.5 ml) with a 0.4-μm separated cell-culture system (Becton–Dickinson). Cellular viability and the number of $CD4^+$ T cells were determined by trypan blue dye exclusion and a cell counter (CDA-500, Sysmex Mundelin, IL, USA), respectively. T cells and DCs were easily distinguishable with each cell size using a cell counter.

2.5. Blocking assay for MHC class II molecules

To examine the effect of MHC class II proteins on Mo-DCs or of exosome preparations on naive $CD4^+$ T cell survival, Mo-DCs (1.0×10^5 cells/ml), crude exosomes, or purified exosomes prepared from 1×10^5 Mo-DC/ml were preincubated with anti-MHC class II mAb (4 μg/ml, Diaclone Research Besaucon, France) at 37 °C for 1 h, and $CD4^+$ T cells (1.0×10^6 cells/ml) were added and cultured at 37 °C for 4 days. Isotype-matched IgG1 mAb was used as a control.

2.6. FACS analysis

A 10× concentrate of crude exosomes (100 μl) was mixed with 100 μl FITC-conjugated anti-HLA-DR mAb and PE-conjugated anti-CD86 mAb. After a 30-min incubation at 4 °C, the samples were diluted with FACS buffer, and the fluorescence intensities of the exosome preparations were measured with a FACS Calibur flow cytometer and were analyzed with CELLQuest software.

Purified exosomes were prepared with human anti-HLA-DP, -DQ, or -DR-coated paramagnetic beads as described above. Purified exosomes (10 μl) were suspended in 100 μl FACS buffer, mixed with FITC-conjugated anti-HLA-DR mAb (10 μl) and PE-conjugated anti-CD86 mAb (10 μl), and incubated at 4 °C for 30 min. The samples were washed twice on a magnetic rack with FACS buffer, followed by reconstitution of the bead pellets in buffer containing 1% formaldehyde. Stained and fixed exosome-coupled beads were analyzed on a FACS Calibur flow cytometer with CELLQuest software.

2.7. Electrophoretic mobility shift assay

NF-κB activity in nuclei isolated from naive $CD4^+$ T cells was determined by electrophoretic mobility shift assay (EMSA). Extraction of nuclear proteins and EMSA were performed as described previously [27]. Briefly, 5 μg of nuclear protein was incubated for 30 min at room temperature with binding buffer (20 mM Hepes–NaOH, pH 7.9, 2 mM EDTA, 100 mM NaCl, 10% glycerol, and 0.2% NP-40), poly(dI–dC), and ^{32}P-labeled double-stranded oligonucleotide containing the NF-κB binding motif (Promega, Madison, WI, USA). The sequence of the double-stranded oligomer used for EMSA is as follows: 5′-AGTTGAGGGGACTTTCCC AGGC-3′ (sense strand). The reaction mixtures were loaded on a 4% polyacrylamide gel and electrophoresed with running buffer 0.25× TBE. After the gel was dried, DNA–protein complexes were visualized by autoradiography.

2.8. Electron microscopy

Exosome-bead complexes were fixed in 3% glutaraldehyde in 0.1 M cacodylate buffer (CB) at pH 7.3 for 3 h at 4 °C and washed in 0.1 M CB. The complexes were resuspended and embedded in 4% agar [28]. After the

agar was cut into 1-mm^3 pieces, the pieces were fixed in 1% osmium tetroxide in 0.1 M CB overnight and washed in distilled water. The specimens were dehydrated in a graded series of ethanol and embedded in Epon 812. Ultrathin sections were treated with uranyl acetate followed by lead citrate and were examined with an electron microscope (JEM-1200EX, JEOL, Tokyo, Japan).

2.9. Statistical analysis

Comparison of means among three or more groups was done by the Scheffé's method. All results with a p value of less than 0.05 were considered statistically significant.

3. Results

3.1. Mo-DCs support naive CD4$^+$ T cell survival

When naive CD4$^+$ T cells were cultured in RPMI medium in the absence of Mo-DCs, CD4$^+$ T cell numbers decreased daily. Coculture of CD4$^+$ T cells with Mo-DCs at a ratio of 10:1 significantly supported CD4$^+$ T cell survival (Fig. 1A). Mo-DCs supported CD4$^+$ T cell survival in a dose-dependent manner (Fig. 1B). Taken together, CD4$^+$ T cells and Mo-DCs were principally used at a cell ratio of 10:1 throughout this study. To examine whether direct contact between CD4$^+$ T cells and Mo-DCs was required to support CD4$^+$ T cell survival, we used a separated cell-culture system as described in Materials and methods. When CD4$^+$ T cells were cultured without direct contact with Mo-DCs, the number of CD4$^+$ T cells decreased compared to that in mixed cultures but increased significantly compared to that of CD4$^+$ T cells alone (Fig. 2A). Because it is believed that small Mo-DC-derived components that can pass through 0.4-μm filters may have a supportive effect on naive CD4$^+$ T cell survival, we speculated that cytokines such as IL-4, IL-7, or IL-15 may be involved. Culture supernatants were filtered with a filter that allows components smaller than 100 kDa to pass through. Both passed (cytokine-rich) and nonpassed (cytokine-poor) fractions were re-adjusted to the original volume with RPMI medium. Contrary to our expectation, the nonpassed fraction but not the passed fraction supported naive CD4$^+$ T cell survival (Fig. 2B).

We next examined which molecules contribute to the prolonged in vitro survival of naive CD4$^+$ T cells. We focused on MHC class II proteins, particularly HLA-DR, which is expressed on Mo-DCs. Pretreatment of Mo-DCs with anti-HLA-DR mAb inhibited the supportive effect on CD4$^+$ T cell survival (Fig. 3A). Interestingly, addition of anti-HLA-DR mAb to the nonpassed fraction also significantly decreased the number of cells (Fig. 3B).

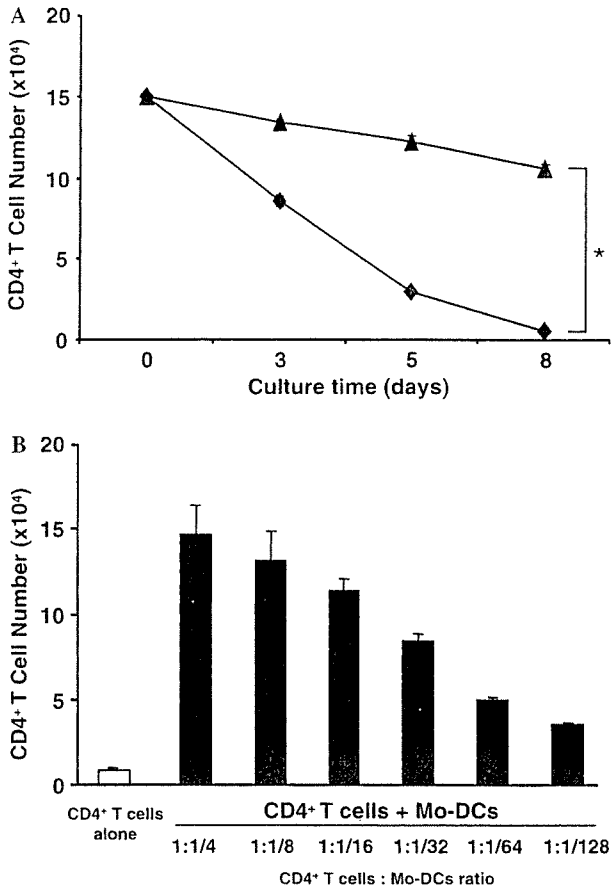

Fig. 1. Coculture with Mo-DCs supports naive CD4$^+$ T cell survival. (A) Purified naive CD4$^+$ T cells were cultured in RPMI medium with (closed triangle) or without (closed diamond) autologous Mo-DCs at a ratio of 10:1. Cell numbers of the viable CD4$^+$ T cells were counted on the indicated days after dead cell exclusion by trypan blue staining. Values represent the means ± SD of triplicate determinations. The asterisk indicates significant differences <0.0001. The data are representative of six independent experiments using Mo-DCs and CD4$^+$ T cells obtained from three different healthy donors. (B) Mo-DCs support naive CD4$^+$ T cell survival in a dose-dependent manner. Purified naive CD4$^+$ T cells (1.5×10^5/150 μl) were cultured with indicated cell numbers of Mo-DCs for 5 days. The data are representative of three independent experiments using Mo-DCs and CD4$^+$ T cells obtained from three different healthy donors.

3.2. Exosomes are present in Mo-DC culture supernatant

We speculated that the HLA-DR-bearing components in the nonpassed fraction may be insoluble substances such as membrane fragments or exosomes. Crude exosomes and purified exosomes were collected from Mo-DC culture supernatants as described in Materials and methods. FACS analysis revealed that 21.5% of the particles in the crude exosomes were positive for both HLA-DR and CD86 (data not shown). The FACS cytogram of purified exosomes coupled to mAb-coated beads showed three populations: single beads, clumps of two beads, and clumps of three or more beads, from the dot-plot representation of forward and side scatter (Fig. 4A-1), as described previously [29]. Single beads represented more

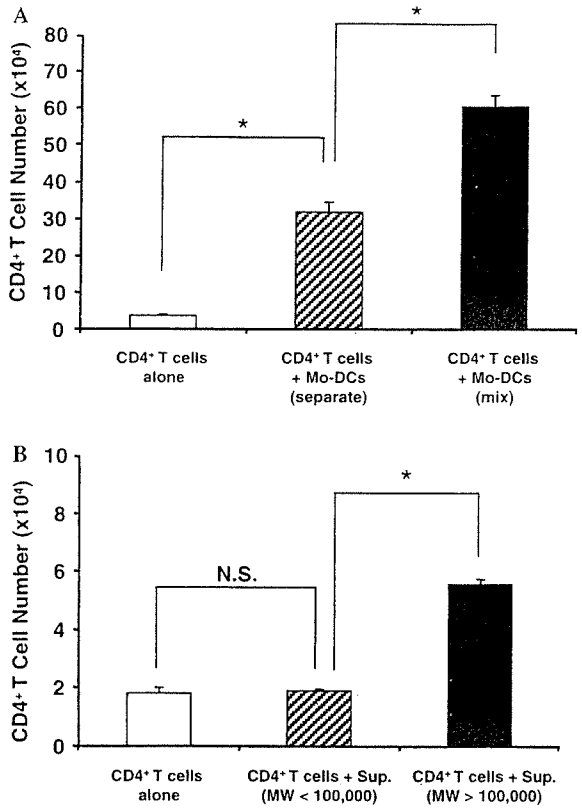

Fig. 2. Supportive effects of Mo-DCs on naive $CD4^+$ T cell survival without direct cellular contact. (A) Viable cell numbers of naive $CD4^+$ T cells cultured in chambers separated by a membrane with pores from Mo-DCs (hatched column) or in the mixture without separation (filled column) were counted on day 5. In only this experiment using separated cell-culture system, $CD4^+$ T cells (1.5×10^6 cells) were cultured with Mo-DCs (1.5×10^5 cells) in 1.5 ml of RPMI medium or were cultured separately in RPMI medium (1.5 ml) with a 0.4-μm separated cell-culture system. Open column shows the cell number of viable naive $CD4^+$ T cells cultured without Mo-DCs. Values represent means ± SD of triplicate determinations. The asterisks indicate significant differences <0.0001. The data are representative of three independent experiments using Mo-DCs and $CD4^+$ T cells obtained from three different healthy donors. (B) Naive $CD4^+$ T cells were cultured in the presence of the culture supernatant of Mo-DCs for 3 days and then the viable cell numbers of the cells were counted. Each column shows the viable cell numbers of the T cells cultured with components smaller than MW 100,000 (hatched column), those larger than MW 100,000 (closed column) or RPMI medium only (open column). Values represent means ± SD of triplicate determinations. The asterisk indicates significant differences 0.0004. N.S. shows not significant. The data are representative of three independent experiments using Mo-DCs and $CD4^+$ T cells obtained from three different healthy donors.

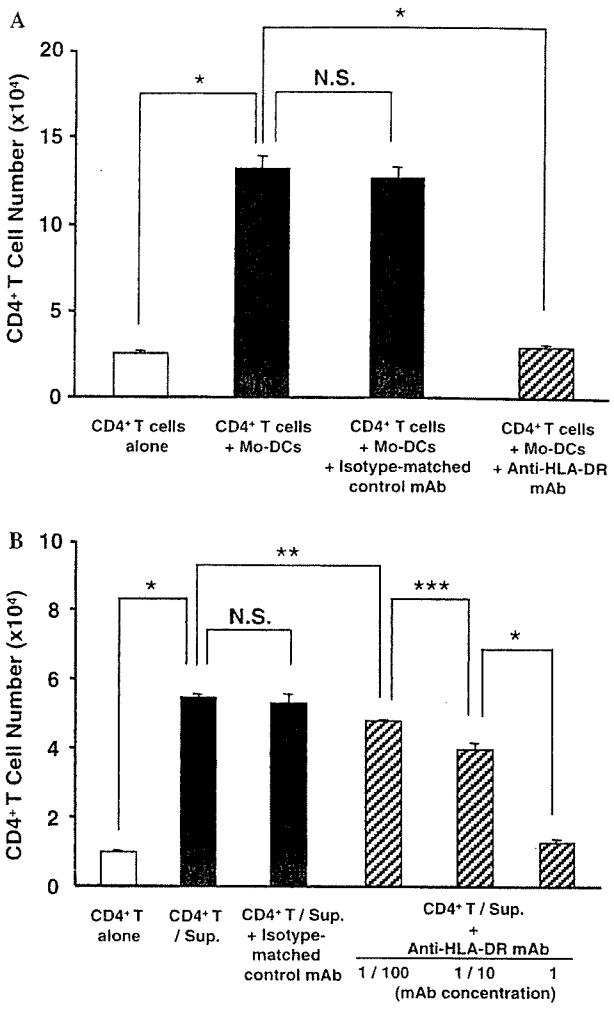

Fig. 3. Requirement of TCR-MHC class II interaction for the prolonged naive $CD4^+$ T cells survival. (A) Viable cell numbers of naive $CD4^+$ T cells cultured with Mo-DCs for 5 days in the presence of anti-MHC class II mAb (4 μg/ml) (hatched column) or isotype-matched control mAb (closed column) were shown. The asterisk indicates significant differences <0.0001. N.S. shows not significant. (B) Naive $CD4^+$ T cells were cultured in the presence of the culture supernatant of Mo-DCs (components of larger than MW 100,000) with anti-MHC class II mAb (hatched column) or with isotype-matched control mAb (closed column) for 4 days and then the viable cell numbers of the cells were counted. The asterisks indicate significant differences <0.0001 (*), 0.002 (**), and 0.007 (***). N.S. shows not significant. Values represent means ± SD of triplicate determinations. The data are representative of three independent experiments using Mo-DCs and $CD4^+$ T cells obtained from three different healthy donors.

than 85% of the total number. The populations containing clumped beads were removed from the analysis by gating for single beads only. More than 90% of the single beads were positive for both HLA-DR and CD86 (Fig. 4A-2). These data indicate that 20% of the particles in the crude exosomes and 90% of the particles in the purified exosomes consist of intact HLA-DR- and CD86-expressing exosomes. Electron microscopic analysis confirmed that the substances coupled to the beads were exosomes (Figs. 4B-1 and B-2). These substances showed the characteristic saucer-like morphology of a flattened sphere limited by a lipid bilayer. The exosomes coupled to the beads ranged from 40 to 140 nm in diameter (means ± SD, 78.46 ± 11.04 nm). The average size of a bead and a $CD4^+$ T cell is 4500 and 7250 nm, respectively.

3.3. Mo-DC-derived exosomes support naive $CD4^+$ T cell survival

To confirm that exosomes are involved in supporting in vitro naive $CD4^+$ T cell survival, purified exosomes

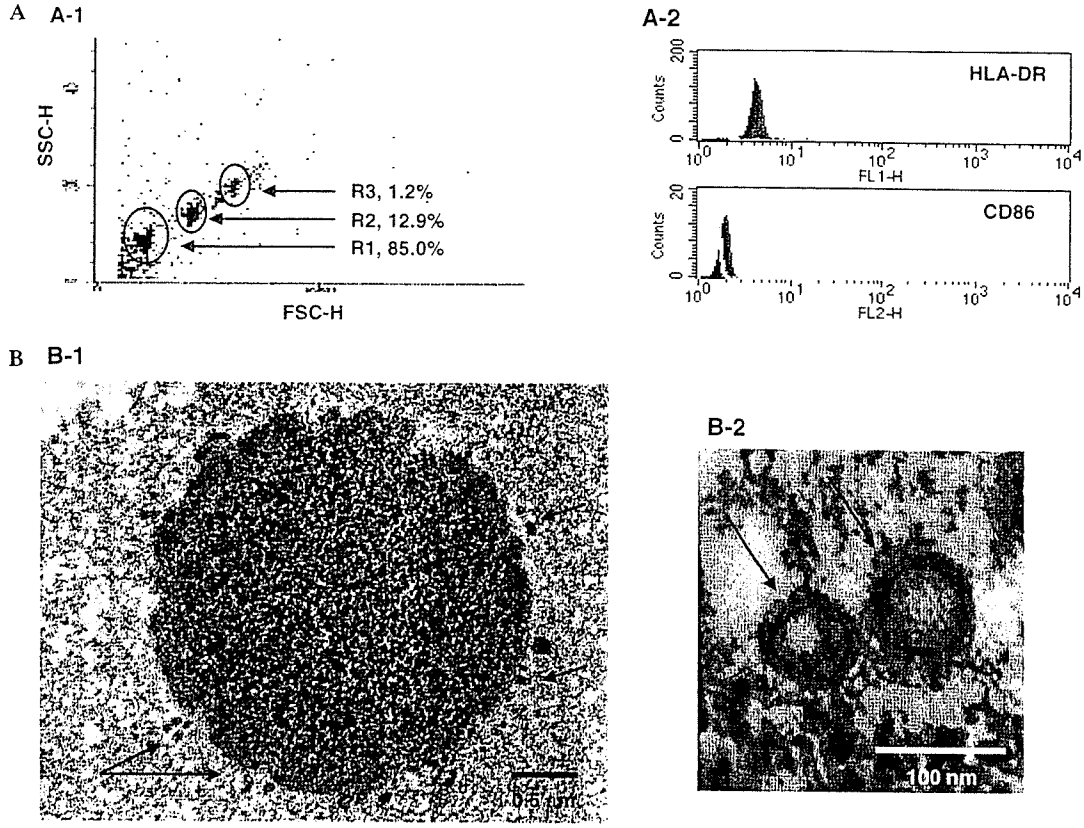

Fig. 4. Detection of MHC class II and CD86 molecules in the components of over MW 100,000 supernatant and electron microscopic characterization of the component. (A) Purified components in supernatants coupled with anti-HLA-DR mAb-coated beads were stained with anti-HLA-DR or anti-CD86 mAbs, and then analyzed by FACS. Three populations of the stained beads appeared in the forward (FSC) and side scatter (SSC) plot are indicated as R1, R2, and R3, respectively and the percentages of each population are also shown (A-1). Histograms show staining of beads for anti-HLA-DR or anti-CD86 (filled line) or control IgG (bold line) on gated R1 area (A-2). The data are representative of three independent experiments. (B) Purified components in supernatants coupled with beads were characterized by electron microscope. Small vesicles (arrows) coating on the surface of the bead (B-1), bar = 0.5 μm and two vesicles of higher magnification (B-2) are shown, bar = 100 nm. The data are representative of six independent experiments using Mo-DCs and $CD4^+$ T cells obtained from three different healthy donors.

coupled to mAb-coated beads were used as effector components. Purified exosomes but not beads alone significantly supported naive $CD4^+$ T cell survival in a dose-dependent manner (Fig. 5A). When beads alone were added to $CD4^+$ T cells, several dying cells were found, and the beads did not bind firmly to any $CD4^+$ T cells. When exosome-coupled beads (purified exosomes) were added to $CD4^+$ T cells, only a few dying cells were found, and the beads bound firmly to several living $CD4^+$ T cells (Fig. 5B). Anti-HLA-DR mAb abrogated the supportive effect of purified exosomes on naive $CD4^+$ T cell survival (Fig. 5C). Anti-HLA-DR mAb also inhibited the binding of exosome-coupled beads to naive $CD4^+$ T cells (data not shown).

3.4. Exosomes induce NF-κB activation in naive $CD4^+$ T cells

We hypothesized that interaction between HLA-DR on exosomes and TCRs on $CD4^+$ T cells induces NF-κB activation, and, as a result, these cells can survive even in severe culture conditions. NF-κB activation of naive $CD4^+$ T cells was estimated by EMSA. Crude exosomes induced NF-κB activation in naive $CD4^+$ T cells within 30 min. Specificity of DNA binding was confirmed by a competition study with a 50-fold excess of unlabeled oligonucleotide. Anti-HLA-DR mAb (4 μg/ml) was added to crude exosomes 1 h prior to coculture with naive $CD4^+$ T cells. Treatment with anti-HLA-DR mAb suppressed exosome-induced NF-κB activation. A NF-κB inhibitor, PDTC (100 μM), was added to naive $CD4^+$ T cells 1 h prior to treatment with crude exosomes. PDTC inhibited nuclear translocation of NF-κB p65 (Fig. 6). PDTC inhibited the supportive effect of crude exosomes on naive $CD4^+$ T cell survival in a dose-dependent manner between 3 and 5 μM without significant direct cytotoxic effect (Fig. 7). These data suggest that exosome-induced NF-κB activation plays a critical role in the survival of naive $CD4^+$ T cells in vitro.

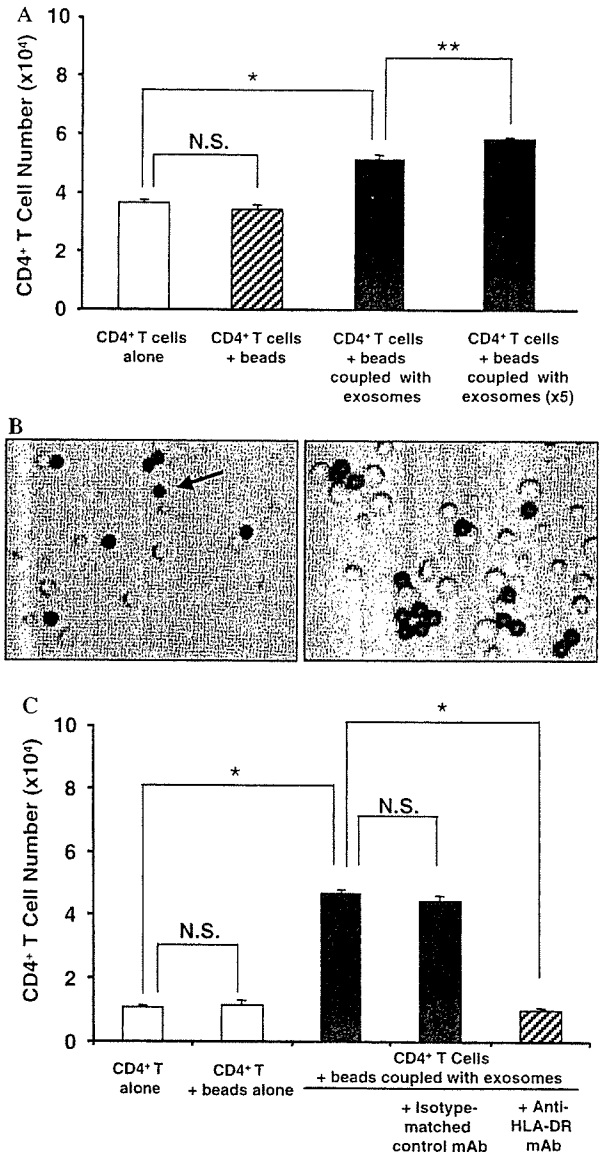

Fig. 5. Prolonged survival of naive CD4$^+$ T cells by interaction with exosomes coupled to anti-MHC class II mAb-coated beads. (A) Viable cell numbers of naive CD4$^+$ T cells cultured with exosomes coupled to anti-MHC class II mAb-coated beads (closed column) for 5 days are shown. Viable cell numbers of CD4$^+$ T cells alone (open column) and CD4$^+$ T cells with anti-HLA-DR mAb-coated beads only (hatched column) are also shown. The asterisk indicates significant differences <0.0001 (*) and 0.0029 (**). N.S. shows not significant. The data are representative of three independent experiments using Mo-DCs and CD4$^+$ T cells obtained from three different healthy donors. (B) Phase-contrast photomicrographs of CD4$^+$ T cells 5 days after coculture with beads (arrow) alone (left panel) and beads coupled with exosomes (right panel). The pictures are representative of three independent experiments using Mo-DCs and CD4$^+$ T cells obtained from three different healthy donors. (C) Viable cell numbers of CD4$^+$ T cells cultured with exosome-coupled beads in the presence (hatched column) or the absence (closed column) of anti-HLA-DR mAb or in the presence (closed column) of isotype-matched control mAb. Open column shows the viable cell number of CD4$^+$ T cells alone and CD4$^+$ T cells cultured with beads alone. The asterisk indicates significant differences <0.0001. N.S. shows not significant. Values represent means ± SD of triplicate determinations. The data are representative of three independent experiments using Mo-DCs and CD4$^+$ T cells obtained from three different healthy donors.

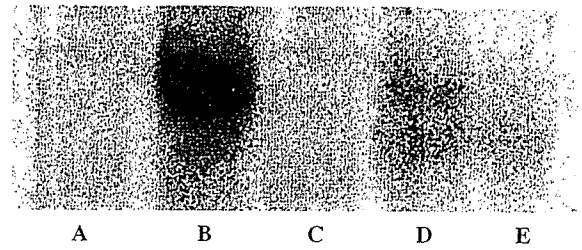

Fig. 6. NF-κB activation in naive CD4$^+$ T cells induced by crude exosomes. The nuclear translocation of NF-κB p65 of naive CD4$^+$ T cells in response to exosomes was determined by EMSA. Naive CD4$^+$ T cells were incubated for 30 min for various conditions as below. Lane A, medium only; lane B, crude exosomes; lane C, crude exosomes with NF-κB ODN (50×); lane D, crude exosomes with anti-HLA-DR mAb; and lane E, crude exosomes with PDTC (100 μM). The data are representative of three independent experiments using Mo-DCs and CD4$^+$ T cells obtained from three different healthy donors.

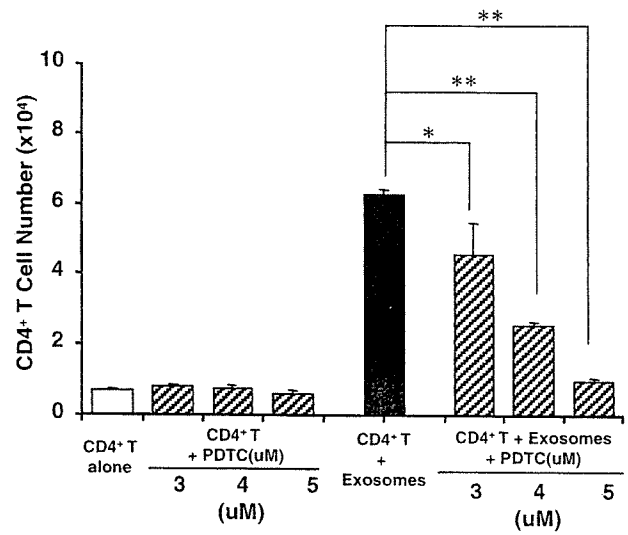

Fig. 7. Suppression of exosome-induced prolonged survival of naive CD4$^+$ T cells by NF-κB inhibitor PDTC. Viable cell numbers of naive CD4$^+$ T cells cultured with crude exosomes (closed column), crude exosomes with indicated concentrations of PDTC (hatched column) or medium alone (open column) for 5 days are shown. The asterisks indicate significant differences 0.0016 (*), <0.0001 (**). Values represent means ± SD of triplicate determinations. The data are representative of three independent experiments using Mo-DCs and CD4$^+$ T cells obtained from three different healthy donors.

4. Discussion

We showed that Mo-DC-derived exosomes can prolong naive CD4$^+$ T cell survival in an HLA-DR-dependent manner. Our data also suggest that NF-κB activation induced by exosomes contributes to this increased survival.

Several players such as TCRs and CD28 are related to T cell survival [5,30]. In the last two decades, many in vivo studies in mice have shown that long-term survival of naive CD4$^+$ T cells requires interaction with self-MHC class II proteins [1–3]. However, it remains

unclear whether interaction with these proteins can prolong the short-term survival of naive $CD4^+$ T cells in vitro. Recently, it was shown that human Mo-DCs expressing abundant MHC class II proteins are able to support short-term survival of T cells in vitro [7]. Interestingly, our present findings indicate that although HLA-DR is critical for naive $CD4^+$ T cell survival in vitro (Fig. 3A), direct interaction between Mo-DCs and T cells is not always required (Fig. 2A). It has been shown that MHC class II proteins are very abundant in exosomes from APCs [10]. In the present study, Mo-DCs also released exosomes into culture medium, and Mo-DC-derived exosomes expressed both MHC class II and CD86 proteins (Fig. 4A). Recently, it was reported that MHC class II proteins on released exosomes are functional [10,31]. Raposo et al. [10] showed that exosomes derived from both human and murine B lymphocytes induce antigen-specific MHC class II-restricted T cell responses. Vincent-Schneider et al. [31] showed that the combination of exosomes with DCs results in highly efficient stimulation of specific T cells and suggested that exosome-bearing MHC class II complexes are taken up by dedicated APCs for efficient T cell activation. On the basis of these findings, we hypothesized that Mo-DC-derived exosomes can prolong naive $CD4^+$ T cell survival. To prove this, we used exosomes purified with human anti-HLA-DP, -DQ, or -DR-coated paramagnetic beads. To avoid contamination with serum-derived exosomes [32], we used RPMI 1640 medium supplemented with 1% human albumin. Purified exosomes prolonged naive $CD4^+$ T cell survival in an HLA-DR-dependent manner (Fig. 5C).

The present study shows a novel function of exosomes. Mo-DC-derived exosomes express not only MHC class II but also CD86 proteins. CD28, which is a ligand for CD86, is believed to contribute to T cell survival [29]. In our study, peripheral monocytes, in which CD86 expression is weak, did not prolong $CD4^+$ T cell survival (data not shown), suggesting a possible role of a CD28/CD86 interaction. But our data that specific antibody against HLA-DR inhibited completely the effect of exosomes on $CD4^+$ T cell survival. These data indicate that TCR is a likely candidate for transmitting the viability signal. However, participation of other receptors for MHC class II such as LAG-3 has not been excluded [33]. Furthermore, other molecular events, such as CD28/CD86 interaction, in addition to the interaction between TCR and HLA-DR may operate in prolongation of $CD4^+$ T cell survival induced with exosomes. A role of exosome-bearing CD86 in $CD4^+$ T cell survival has not been reported, and the mechanism of exosome-induced, HLA-DR-dependent naive $CD4^+$ T cell survival is not clear. Several transcription factors such as Ets, NFAT, AP-1, and NF-κB have been shown to be activated by TCRs or CD28 [20]. Recent studies have indicated that NF-κB plays a key role in T cell survival. For example, it has been suggested that the PI3K/Akt pathway is important for the effects of both CD28 and IL-2R [23,34,35], and NF-κB is thought to be target of Akt [36,37]. More direct evidence that NF-κB contributes to T cell survival has been reported recently [22,26]. In p50−/− cRel−/− mice, which exhibit virtually no inducible κB site binding activity, an essential role of TCR-induced NF-κB was indicated in T cell survival [26]. In addition, NF-κB regulated TCR-induced expression of anti-apoptotic Bcl-2 family members and NF-κB activation was not only necessary but was also sufficient for T cell survival [38]. Wan and DeGregon [22] reported that the survival of antigen-stimulated T cells requires NF-κB-mediated inhibition of p73 expression. Our present data show for the first time that Mo-DC-derived exosomes can induce NF-κB activation in naive $CD4^+$ T cells (Fig. 6). PDTC is a stable analog of dithiocarbamate and is one of the most widely used inhibitors of NF-κB signaling [39]. Although it has been postulated that PDTC acts simply as an antioxidant to inhibit NF-κB activation [40], it has been shown definitively that PDTC inhibits NF-κB activation independently of antioxidative function [41]. In the present study, we used PDTC to examine contribution of the NF-κB pathway to exosome-mediated $CD4^+$ T cell survival. PDTC inhibited the supportive effect of exosomes on $CD4^+$ T cell survival in a dose-dependent manner without significant direct cytotoxic effect (Fig. 7). These results suggest that NF-κB plays an essential role in exosome-mediated $CD4^+$ T cell survival. However, we have no definitive evidence as to how exosomes induce NF-κB in naive $CD4^+$ T cells.

It has been reported that DC-derived exosomes may be used as vectors for vaccination because they express high levels of functional MHC class I– and class II–peptide complexes, together with CD86 [10,14,19]. A recent report showed that MHC class I proteins on purified exosomes from DCs can be directly loaded with peptide at much greater levels than by indirect loading [17]. Also reported was a new exosome purification procedure from Mo-DCs [14], in which ultrafiltration through a 500-kDa membrane and ultracentrifugation into a 30% sucrose/deuterium-oxide cushion made it possible to recover up to 50% exosomes. Although the function of most of the exosome-bearing proteins is unknown at present, accumulated data on exosome function suggest that these proteins will become exciting therapeutic tools in the near future.

Acknowledgments

We thank Yasuhiro Hirakawa (Department of Anatomy and Cell Biology affiliation), Takaaki Kanemaru, and Kaori Nomiyama for technical assistance.

References

[1] S. Takeda, H.R. Rodewald, H. Arakawa, H. Bluethmann, T. Shimizu, MHC class II molecules are not required for survival of newly generated CD4+ T cells, but affect their long-term life span, Immunity 5 (1996) 217–228.

[2] T. Brocker, Survival of mature CD4 T lymphocytes is dependent on major histocompatibility complex class II-expressing dendritic cells, J. Exp. Med. 186 (1997) 1223–1232.

[3] S. Garcia, J. DiSanto, B. Stockinger, Following the development of a CD4 T cell response in vivo: from activation to memory formation, Immunity 1 (1999) 163–171.

[4] C. Tanchot, F.A. Lemonnier, B. Perarnau, A.A. Freitas, B. Rocha, Differential requirements for survival and proliferation of CD8 naive or memory T cells, Science 276 (1997) 2057–2062.

[5] J. Kirberg, A. Berns, H. von Boehmer, Peripheral T cell survival requires continual ligation of the T cell receptor to major histocompatibility complex-encoded molecules, J. Exp. Med. 186 (1997) 1269–1275.

[6] C. Viret, F.S. Wong, C.A. Janeway Jr., Designing and maintaining the mature TCR repertoire: the continuum of self-peptide:self-MHC complex recognition, Immunity 10 (1999) 559–568.

[7] T. Kondo, I. Cortese, S. Markovic-Plese, K.P. Wandinger, C. Carter, M. Brown, S. Leitman, R. Martin, Dendritic cells signal T cells in the absence of exogenous antigen, Nat. Immunol. 2 (2001) 932–938.

[8] E.G. Trams, C.J. Lauter, N. Salem Jr., U. Heine, Exfoliation of membrane ecto-enzymes in the form of micro-vesicles, Biochim. Biophys. Acta 645 (1981) 63–70.

[9] R.M. Johnstone, M. Adam, J.R. Hammond, L. Orr, C. Turbide, Vesicle formation during reticulocyte maturation. Association of plasma membrane activities with released vesicles (exosomes), J. Biol. Chem. 262 (1987) 9412–9420.

[10] G. Raposo, H.W. Nijman, W. Stoorvogel, R. Liejendekker, C.V. Harding, C.J. Melief, H.J. Geuze, B lymphocytes secrete antigen-presenting vesicles, J. Exp. Med. 183 (1996) 1161–1172.

[11] J.Q. Davis, D. Dansereau, R.M. Johnstone, V. Bennett, Selective externalization of an ATP-binding protein structurally related to the clathrin-uncoating ATPase/heat shock protein in vesicles containing terminal transferrin receptors during reticulocyte maturation, J. Biol. Chem. 261 (1986) 15368–15371.

[12] C. Thery, M. Boussac, P. Veron, P. Ricciardi-Castagnoli, G. Raposo, J. Garin, S. Amigorena, Proteomic analysis of dendritic cell-derived exosomes: a secreted subcellular compartment distinct from apoptotic vesicles, J. Immunol. 166 (2001) 7309–7318.

[13] F. Sallusto, A. Lanzavecchia, Efficient presentation of soluble antigen by cultured human dendritic cells is maintained by granulocyte/macrophage colony-stimulating factor plus interleukin 4 and downregulated by tumor necrosis factor alpha, J. Exp. Med. 179 (1994) 1109–1118.

[14] L. Zitvogel, A. Regnault, A. Lozier, J. Wolfers, C. Flament, D. Tenza, P. Ricciardi-Castagnoli, G. Raposo, S. Amigorena, Eradication of established murine tumors using a novel cell-free vaccine: dendritic cell-derived exosomes, Nat. Med. 4 (1998) 594–600.

[15] H.G. Lamparski, A. Metha-Damani, J.Y. Yao, S. Patel, D.H. Hsu, C. Ruegg, J.B. Le Pecq, Production and characterization of clinical grade exosomes derived from dendritic cells, J. Immunol. Methods 270 (2002) 211–226.

[16] C. Thery, L. Duban, E. Segura, P. Veron, O. Lantz, S. Amigorena, Indirect activation of naive CD4+ T cells by dendritic cell-derived exosomes, Nat. Immunol. 3 (2002) 1156–1162.

[17] D.H. Hsu, P. Paz, G. Villaflor, A. Rivas, A. Mehta-Damani, E. Angevin, L. Zitvogel, J.B. Le Pecq, Exosomes as a tumor vaccine: enhancing potency through direct loading of antigenic peptides, J. Immunother. 26 (2003) 440–450.

[18] I. Hwang, X. Shen, J. Sprent, Direct stimulation of naive T cells by membrane vesicles from antigen-presenting cells: distinct roles for CD54 and B7 molecules, Proc. Natl. Acad. Sci. USA 100 (2003) 6670–6675.

[19] D. Skokos, H.G. Botros, C. Demeure, J. Morin, R. Peronet, G. Birkenmeier, S. Boudaly, S. Mecheri, Mast cell-derived exosomes induce phenotypic and functional maturation of dendritic cells and elicit specific immune responses in vivo, J. Immunol. 170 (2003) 3037–3045.

[20] C.T. Kou, J.M. Leiden, Transcriptional regulation of T lymphocyte development and function, Annu. Rev. Immunol. 17 (1999) 149–187.

[21] E. Dudley, F. Hornung, L. Zheng, D. Scherer, D. Ballard, M. Lenardo, NF-kappaB regulates Fas/APO-1/CD95- and TCR-mediated apoptosis of T lymphocytes, Eur. J. Immunol. 29 (1999) 878–886.

[22] Y.Y. Wan, J. DeGregon, The survival of antigen-stimulated T cells requires NFkappaB-mediated inhibition of p73 expression, Immunity 18 (2003) 331–342.

[23] R.G. Jones, M. Parsons, M. Bonnard, V.S. Chan, W.C. Yeh, J.R. Woodgett, P.S. Ohashi, Protein kinase B regulates T lymphocyte survival, nuclear factor kappaB activation, and Bcl-X(L) levels in vivo, J. Exp. Med. 191 (2000) 1721–1734.

[24] S. Ghosh, M.J. May, E.B. Kopp, NF-kB and Rel proteins: evolutionarily conserved mediators of immune responses, Annu. Rev. Immunol. 16 (1998) 225–260.

[25] J.A. DiDonato, F. Mercurio, M. Karin, Phosphorylation of IkB precedes but is not sufficient for its dissociation from NF-kB, Mol. Cell. Biol. 15 (1995) 1302–1311.

[26] Y. Zheng, M. Vig, J. Lyons, L. Van Parijs, A.A. Bed, Combined deficiency of p50 and cRel in CD4+ T cells reveals an essential requirement for nuclear factor kappa B in regulating mature T cell survival and in vivo function, J. Exp. Med. 197 (2003) 861–874.

[27] M. Kojima, T. Morisaki, K. Izuhara, A. Uchiyama, Y. Matsunari, M. Katano, M. Tanaka, Lipopolysaccharide increase cyclooxygenase-2 expression in a colon carcinoma cell line through nuclear factor-kappa B activation, Oncogene 19 (2000) 1225–1231.

[28] J.A. Hobot, E. Carlemalm, W. Villiger, E. Kellenberger, Periplasmic gel: new concept resulting from the reinvestigation of bacterial cell envelope ultrastructure by new methods, J. Bacteriol. 160 (1984) 143–152.

[29] A. Clayton, J. Court, H. Navabi, M. Adams, M.D. Mason, J.A. Hobot, G.R. Newman, B. Jasani, Analysis of antigen presenting cell derived exosomes, based on immuno-magnetic isolation and flow cytometry, J. Immunol. Methods 247 (2001) 163–174.

[30] L.H. Boise, A.J. Minn, P.J. Noel, C.H. June, M.A. Accavitti, T. Lindsten, C.B. Thompson, CD28 costimulation can promote T cell survival by enhancing the expression of Bcl-XL, Immunity 3 (1995) 87–98.

[31] H. Vincent-Schneider, P. Stumptner-Cuvelette, D. Lankar, S. Pain, G. Raposo, P. Benaroch, C. Bonnerot, Exosomes bearing HLA-DR1 molecules need dendritic cells to efficiently stimulate specific T cells, Int. Immunol. 14 (2002) 713–722.

[32] G. van Niel, G. Raposo, C. Candalh, M. Boussac, R. Hershberg, N. Cerf-Bensussan, M. Heyman, Intestinal epithelial cells secrete exosome-like vesicles, Gastroenterology 121 (2001) 337–349.

[33] C.J. Workman, D.A. Vignali, The CD4-related molecule, LAG-3 (CD223), regulates the expansion of activated T cells, Eur. J. Immunol. 33 (2003) 970–979.

[34] J.S. Burr, N.D. Savage, G.E. Messah, S.L. Kimzey, A.S. Shaw, R.H. Arch, J.M. Green, Cutting edge: distinct motifs within CD28 regulate T cell proliferation and induction of Bcl-XL, J. Immunol. 166 (2001) 5331–5335.

[35] K.A. Frauwirth, J.L. Riely, M.H. Harris, R.V. Parry, J.C. Rathmell, D.R. Plas, R.L. Elstrom, C.H. June, C.B. Thompson, The CD28 signaling pathway regulates glucose metabolism, Immunity 16 (2002) 769–777.

[36] L.P. Kane, V.S. Shapiro, D. Stokoe, A. Weiss, Induction of NF-kappaB by the Akt/PKB kinase, Curr. Biol. 9 (1999) 601–604.
[37] J.A. Romashkova, S.S. Makarov, NF-kappaB is a target of AKT in anti-apoptotic PDGF signaling, Nature 401 (1999) 86–90.
[38] R.J. Grumont, I.J. Rourke, S. Gerondakis, Rel-dependent induction of A1 transcription is required to protect B cells from antigen receptor ligation-induced apoptosis, Genes Dev. 13 (1999) 400–411.
[39] P.A. Baeuerle, T. Henkel, Function and activation of NF-kB in the immune system, Annu. Rev. Immunol. 12 (1994) 141–179.
[40] L. Flohe, R. Brigelius-Flohe, C. Saliou, M.G. Traber, L. Packer, Redox regulation of NF-kappa B activation, Free Radic. Biol. Med. 22 (1997) 1115–1126.
[41] M. Hayakawa, H. Miyashita, I. Sakamoto, M. Kitagawa, H. Tanaka, H. Yasuda, M. Karin, K. Kikugawa, Evidence that reactive oxygen species do not mediate NF-kB activation, EMBO J. 22 (2003) 3356–3366.

Dendritic-cell therapy after non-myeloablative stem-cell transplantation for renal-cell carcinoma

Katsunori Tatsugami, Masatoshi Eto, Masahiko Harano, Koji Nagafuji, Kazuya Omoto, Mitsuo Katano, Mine Harada, and Seiji Naito

Lancet Oncol 2004; **5**: 750–52

Treatment of advanced renal-cell carcinoma is generally by nephrectomy before systemic therapy, even in patients with metastatic disease. Most patients with metastasis are treated with interferon alfa and interleukin 2 after surgery because advanced renal-cell carcinoma is highly resistant to chemotherapy and radiotherapy. However, studies have shown that non-myeloablative allogeneic peripheral-blood stem-cell transplantation leads to a graft-versus-tumour effect in patients with metastatic renal-cell carcinoma.[1,2]

A 56-year-old man underwent a radical nephrectomy for a right renal tumour in July, 1998. Histopathological analysis showed renal-cell carcinoma of clear-cell type. 2 years after surgery, the patient developed metastasis in the lung and bone, and was subsequently given immunotherapy with interferon alfa and interleukin 2. However, the metastasis progressed during immunotherapy and the patient underwent a non-myeloablative allogeneic peripheral-blood stem-cell transplantation in October, 2002. The day of infusion of donor cells was called day 0 in this protocol. The

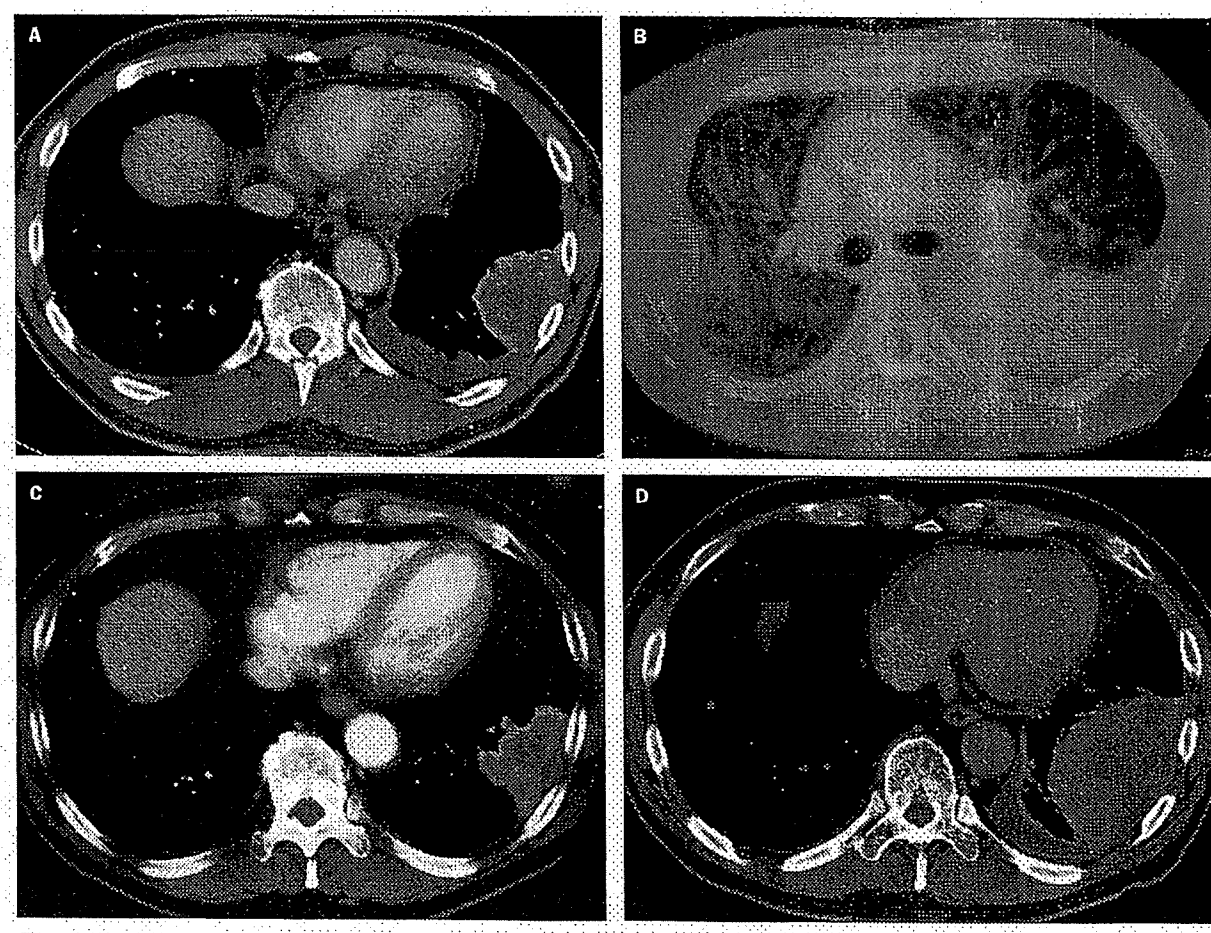

Figure 1: Clinical course of transplantation. A: Lung metastasis and pleural effusion before transplantation. B: Chest CT scan shows ground glass opacity 72 days after transplantation. C: No presence of pleural effusion or lesion 155 days after transplantation. D: Tumour growth 340 days after transplantation.

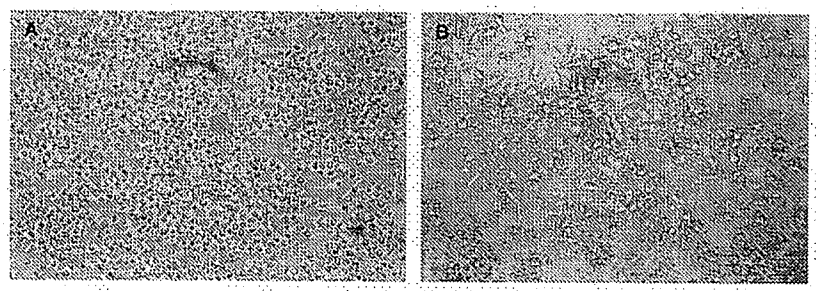

Figure 2. Microscopic analysis of monocytes after stimulation with tumour necrosis factor alfa and dinoprostone. Stimulated monocytes from the patient (A) show no dendritic shape compared with donor monocytes (B).

patient received 30 mg/m² per day fludarabine from day 8 before donor-cell infusion to day 3 before infusion; 4 mg/kg busulfan on days 6 and 5 before infusion; 3 mg/kg ciclosporin the day before infusion; and an infusion of 5×10^6/kg CD34-positive cells on the day of infusion from a donor sibling with a mismatch at a single HLA locus. 5 mg/m² methotrexate was given on days 1, 3, and 6 after donor-cell infusion and the patient also received 3 mg/kg ciclosporin daily after transplantation to prevent acute graft-versus-host disease.

The patient showed mixed chimerism for a short period and as a result we lowered the concentration of ciclosporin, which resulted in the onset of graft-versus-host disease. 70 days after the transplantation, the patient had dry eyes, a cough, and dyspnoea. Chest CT showed ground glass opacity and pleural effusion compatible with interstitial pneumonia (figure 1B), which was treated by steroid-pulse therapy (1 g methylprednisolone for 3 days). After the onset of severe graft-versus-host disease, the recipient's peripheral-blood cells changed completely into donor-type cells. Although the tumour continued to grow for 3 months after myelosuppressive treatment, tumour effusion and pleural effusion decreased after the onset of graft-versus-host disease (figure 1A and 1C). However, to control the graft-versus-host disease, the patient continued immunosuppressive therapy with 5–15 mg predonisolone daily and 25 mg ciclosporin daily for over 1 year, the tumour regrew 11 months after transplantation (figure 1D).

Interferon alfa or interleukin 2 has been given to patients who had progressive disease after transplantation[1] In some patients who receive immunosuppressive treatment to control severe graft-versus-host disease, use of interferon alfa and interleukin 2 after transplantation might enhance the graft-versus-host disease elicited by the allograft. Several clinical trials[3,4] have established the safety and feasibility of immunotherapy with dendritic cells, which can elicit specific antitumour immune responses and some clinically meaningful responses. Furthermore, no serious adverse effects or clinical signs of an autoimmune reaction were recorded in these trials. Therefore, we attempted give this patient immunotherapy by use of dendritic cells.

This immunotherapeutic technique used monocytes extracted from peripheral-blood cells of the patient. At the time of monocyte extraction, laboratory analysis showed a high concentration of C-reactive protein (72·4 mg/L) and mild anaemia (red-cell count $3\cdot0\times10^{12}$/L, haemoglobin 1·37 mmol/L). White-cell count was within the normal range ($7\cdot07\times10^9$/L). All monocytes from the patient were thought to be derived from the donor cells because complete chimerism had been already established in the patient. Monocytes were cultured in RPMI1640 medium supplemented with 5% human serum albumin in the presence of 100 μg/L molgramostim and 50 μg/L interleukin 4 for 7 days. The culture medium was changed on day 3. On day 7 the dendritic cells were pulsed with 100 mg/L autologous tumour lysate overnight and stimulated with 200 U/mL tumour necrosis factor alfa and 1 mg/L dinoprostone for 2 days. Because preliminary experiments showed that the maturation of dendritic cells from the monocytes of the patient was inadequate, we compared the dendritic-cell maturation of the patient's cells with that of the donor cells. Analysis of the shape and phenotypes of the cultured cells after stimulation with tumour necrosis factor alfa and dinoprostone showed that stimulated monocytes from the patient were smaller than those from the donor, and that no dendrites were present after stimulation (figure 2A). We then confirmed the phenotype of the cells by flow cytometry: staining of stimulated cells with CD83 molecules (monocyte markers), and analysis of forward scatter and side scatter showed a lower number of large cells such as dendritic cells in the patient's sample than in the donor sample for CD83-positive cells. Mature dendritic cells usually highly express MHC class II molecules and costimulatory molecules such as CD80 or CD86. However, the CD83-positive cells from the patient showed low expression of MHC class II, CD80, and CD86 after stimulation (figure 2B and figure 3). These results suggest that monocytes from the patient poorly differentiated into dendritic cells. Thus, we scheduled immunotherapy with dendritic cells derived from the donor's peripheral-blood cells. $1\cdot0–3\cdot9\times10^7$ mature dendritic cells pulsed with tumour lysate (100 mg/L) were given intradermally every week for 5 weeks and every other week for a further 4 weeks. The patient had no serious adverse effects apart from high-grade fever of 39°C after injection. Although immunotherapy with dendritic cells was safe for this patient, we could not inhibit the tumour growth without inducing

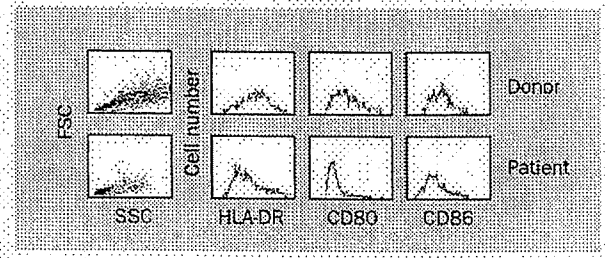

Figure 3. Phenotype of CD83-positive cells after stimulation. Number of large cells with a dendritic-cell phenotype from the patient was lower than that from the donor according to forward scatter (FSC) and side scatter (SSC). CD83-positive cells from the donor highly expressed HLA-DR, CD80, and CD86 after stimulation.